Calhoun

Institutional Archive of the Naval Postgraduate School

Calhoun: The NPS Institutional Archive

DSpace Repository

Theses and Dissertations 1. Thesis and Dissertation Collection, all items

1952-06

Determination of the longitudinal and lateral stability derivatives of the Stinson L-5 airplane from steady state flight tests

Saldin, Carl N.; Kurtz, William E.

Princeton University

http://hdl.handle.net/10945/24661

Downloaded from NPS Archive: Calhoun

DUDLEY KNOX LIBRARY

http://www.nps.edu/library

Calhoun is the Naval Postgraduate School's public access digital repository for research materials and institutional publications created by the NPS community. Calhoun is named for Professor of Mathematics Guy K. Calhoun, NPS's first appointed -- and published -- scholarly author.

Dudley Knox Library / Naval Postgraduate School
411 Dyer Road / 1 University Circle
Monterey, California USA 93943

THESIS
S153

DETERMINATION OF THE LONGITUDINAL AND LATERAL STABILITY DERIVATIVES OF THE STINSON L-5 AIRPLANE FROM STEADY STATE FLIGHT TESTS

by
C. N. SALDIN
W. E. KURTZ

Library
U. S. Naval Postgraduate School
Monterey, California

PRINCETON UNIVERSITY

AERONAUTICAL ENGINEERING LABORATORY

Report No. 197

Thesis
S153

THESIS
S153

DETERMINATION OF THE LONGITUDINAL AND LATERAL STABILITY DERIVATIVES OF THE STINSON L-5 AIRPLANE FROM STEADY STATE FLIGHT TESTS

Thesis
S153

ACKNOWLEDGEMENT

The authors wish to express their appreciation to Professor Edward Seckel, under whose direction this investigation was conducted. His ideas, criticisms and suggestions were most helpful for the project.

TABLE OF CONTENTS

Page

I INTRODUCTION 6

II EQUIPMENT 8

III PROCEDURE 10

A. Longitudinal 10

B. Lateral 11

IV RESULTS AND DISCUSSION 13

A. Longitudinal 13

B. Lateral 25

V CONCLUSIONS 36

VI RECOMMENDATIONS 38

VII REFERENCES 39

VIII FIGURES 40

IX APPENDIX 59

I Description and dimensions of the Stinson L-5 59

II Weight and Balance 61

III Symbols and sign convention 64

IV Strain gauge, strain gauge wiring network and calibration 66

V Photographs 67

SUMMARY

The longitudinal and lateral stability derivatives for the Stinson L-5 airplane were obtained from non-oscillatory steady state flight technique as described in Reference 1. These derivatives are $C_{n_{\delta_e}}$, $C_{md\theta}$, $C_{n_{\delta_r}}$, $C_{l_{\delta_a}}$, C_{n_r}, C_{y_β}, C_{n_β}, C_{l_β}, $C_{y_{\delta_r}}$, $C_{l_{\delta_r}}$, and $C_{n_{\delta_a}}$. The values of these derivatives, obtained from flight test, are compared with the values of these parameters computed from theoretical formulae where possible. The comparison of the flight test and theoretical results presented a criterion of the effectiveness of the steady state flight technique for determining stability derivatives.

The damping in roll, C_{l_p}, was not determined due to the lack of the necessary equipment.

OBJECT

The object of this investigation was to determine the lateral and longitudinal stability derivatives of the Stinson L-5 airplane using the non-oscillatory steady state flight test technique. By comparing the experimental values of these derivatives with values calculated by means of the theoretical approach, it is hoped that some evaluation of the flight test techniques employed can be made.

DATE AND PLACE OF INVESTIGATION

This study was conducted during the period extending from January to May, 1952 at Princeton University, Princeton, New Jersey. Equipment and facilities of the Aeronautical Engineering Department were used.

INTRODUCTION

Flight testing of airplanes for their aerodynamic characteristics is usually done in one of three distinct methods; namely, the steady state frequency response testing, the transient response testing and the non-oscillatory steady state flight testing. Measuring the frequency response of an airplane to its controls by the steady oscillation technique or the deduction of the frequency response, from the transient response technique, requires a great deal of expensive instrumentation of a complicated nature and accurate data reduction. Exact knowledge of the airplane's mass and inertia characteristics further complicates the frequency response method. On the other hand, non-oscillatory steady state flight testing requires a minimum of simple low cost instrumentation and enables a more precise data reduction. However, the flight time needed to obtain steady state data may preclude its use to airplanes of short endurance; whereas, the flight time needed for each frequency, using oscillatory techniques, is relatively short.

The Stinson L-5 of this investigation, or any of the conventional airplanes, is well suited for the non-oscillatory steady state flight technique of testing. It is with some of these procedures that this investigation will deal.

The longitudinal stability derivatives, elevator power and damping in pitch, are determined from unaccelerated and accelerated flight trim curves. An attempt was made to show the variation of these derivatives with the pitching velocity of the airplane and to explain their changes shown when plotted at various lift coefficients.

Lateral derivatives are determined from skidding turns and steady sideslip maneuvers. Known moments, introduced by use of a towed drogue and a wing weight, are used to determine rudder power and aileron power, respectively. The damping in roll was not determined due to the unavailability of a rate of roll instrument.

Comparison with results computed from analytical equations gives some insight as to the accuracy and usefulness of this method of determining stability derivatives.

EQUIPMENT

The instrumentation used for this investigation is listed and described below. All of the instruments were calibrated by standard procedures.

1. Airspeed Indicator:

The airspeed indicator was a standard sensitive type instrument connected to a full swiveling pitot-static head.

2. Altimeter:

The altitude was measured by a standard sensitive type altimeter.

3. Accelerometer:

The accelerometer consisted of a glass tube 20 inches long, a small coiled spring and a 75 gram steel weight. One end of the spring was attached to the top of the glass tube and the free end was attached to the weight. Both ends of the tube were sealed to provide damping. This instrument was calibrated with a correction considered for the mass of the spring.

4. Elevator, Rudder and Aileron Indicators:

These instruments were controlled by 26-volt, 400 cycle a-c autosyn transmitters linked to the respective control cables. The autosyn followers were calibrated to give the control deflections in degrees.

5. Yaw Indicator:

A yaw meter was attached to the port wing with a boom extending one chord length ahead of the leading edge. The yaw vane was geared to a 24 volt, 400 cycle a-c autosyn transmitter. The autosyn follower was calibrated to give angle of yaw in degrees.

6. Strain Gauge Measuring Device:

This instrument was used to measure the drag of a towed drogue. It consisted of a bridge circuit having four strain gauges mounted on a steel ring. The ring assembly was mounted on the lift strut fitting and was connected to the drogue tow line by the cockpit-controlled release. Static weights were used in the calibration of this system. Appendix IV contains the wiring diagram, strain gauge sketch and the calibration chart.

PROCEDURE

Airplane control powers are the most important aerodynamic characteristics or derivatives that must be determined accurately by flight testing. The major flying controls are the elevator, rudder and ailerons. They produce pitching, yawing and rolling moments, respectively, proportional to their control power. Once the control powers are determined other stability derivatives can be accurately evaluated. In some cases the controls cause secondary moments that have a marked effect on the values determined for certain derivatives.

Longitudinal

The flight test data needed to evaluate the elevator power, C_{m_δ} , and the damping in pitch, $C_{m_{d\theta}}$, is very similar for both derivatives. The elevator power requires curves of elevator angle versus equivalent airspeed for several center of gravity locations. The damping in pitch of the airplane is determined from the same data with additional trim curves for accelerated flight paths. Accelerated flight, in a steady banked turn, establishes a rate of pitch about the Y-axis.

The three center of gravity locations used for the longitudinal flight testing are computed and shown in Appendix II. These c.g. positions were numbered consecutively with #1 c.g. being the most forward. They were obtained by fixing external weights on the fuselage near the tail. The speed range, starting at the stall and going to 130 m.p.h. indicated, was limited by engine RPM. Constant power, estimated at 75% normal rated, was used during these tests. However, the power did

vary slightly as the airplane was climbed or dived to maintain the desired airspeed. To eliminate the elevator tab effect the tab was trimmed to zero deflection for all longitudinal tests.

Plots of the flight data taken for these tests are shown in Figures 1, 2 and 3 as curves of δ_e versus V_e. The 1.4g and 1.6g data was somewhat difficult to obtain at speeds from 80 to 100 m.p.h. due to the slipstream being encountered in the circular flight path. To get the best possible data the flights were made at sunrise and shortly thereafter to avoid any turbulance of the air.

Lateral

The lateral stability derivatives were determined by performing two non-oscillatory steady state flight maneuvers. First, a straight sideslip was flown in which the aileron angle, rudder angle and angle of bank were measured at various angles of sideslip. Second, a skidding turn maneuver was flown in which the aileron angle, rudder angle and rate of turn, $\dot{\psi}$, were measured for various angles of sideslip. These maneuvers were performed at an altitude of 3000 feet at an equivalent airspeed of 100 miles per hour using seventy-five per cent of the normal horsepower.

At high angles of sideslip, during both of these maneuvers, momentary engine failures were encountered due to the loss of fuel flow. The fuel flow difficulty was possibly caused by a vacumn created at the fuel vent tubes or the sticking of the carburetor float valve due to wear in the float hinge. This situation discouraged extensive investigation of lateral flight at other speeds.

The straight sideslip maneuver was performed by use of the directional gyro to maintain a heading. This technique was used for three configurations; namely, the airplane "clean", a weight on the right wing lift strut and a sleeve-drogue attached to the right wing strut. Figures 4, 5 and 6 show the plotted data of these tests. To provide a known torque about the X-axis, a weight was attached to the right wing at 9.05 feet from the X-axis. A dimensionally similar piece of wood was attached to the same station on the left wing giving a net weight of 29 pounds on the right wing. This configuration was used to determine the aileron power. The third configuration consisted of attaching a sleeve-drogue, having the necessary strain gauge components, to the right wing lift strut at a distance of 9.075 feet from the X-axis to introduce a known yawing moment about the Z-axis. Prior calibration of the strain gauge enabled the determination of the actual drag at the moment of the test. The drag was found to be 41 pounds. Rudder control power was determined from the data obtained during testing this flight configuration.

The skidding turn technique was performed by use of the gyro horizon to maintain a wing level attitude of the airplane. Plotted on Figure 7 are the control deflections measured at each sideslip angle during this maneuver. To determine the rate of turn, $\dot{\psi}$, the airplane was timed through an observed number of degrees turn on the directional gyro. This method is liable to error but sufficient data was taken to establish a correct slope. The results of turning rate versus angle of sideslip are shown on Figure 8.

RESULTS AND DISCUSSION

Longitudinal

$C_{m_{\delta_e}}$:

An airplane is in equilibrium if the sum of the moments acting upon it, about any chosen reference line, is zero. When the airplane is tested at three different center of gravity locations, it will produce as many different moments about a given reference line due to the weight shift. In flight these moments, acting on the airplane in the longitudinal plane, must be balanced by a moment produced by the deflected elevator. The deflection of the elevator changes the effective angle of attack of the horizontal tail, thus changing the tail lift; the result is a moment about the reference axis. The magnitude of the pitching moment coefficient produced by the control, per degree deflection, is a measure of the elevator power, $C_{m_{\delta_e}}$.

For this investigation the elevator power was evaluated from flight data by three methods. The first method is considered approximate and is described in Reference 1. If the assumption that the airplane lift coefficient equals the wing lift coefficient is made, the moment equation about the Y-axis becomes:

$$C_{m_{\delta_e}} \Delta\delta_e + C_{L_a} \frac{\Delta x_a}{c} = 0$$

$$C_{m_{\delta_e}} = - C_{L_a} \frac{\Delta x_a}{c} \Big/ \Delta\delta_e$$

From the unaccelerated stick fixed trim curves of elevator angle versus equivalent airspeed for the three c.g. locations, plots of δ_e versus C_{l_a}

were made as indicated by Figure 9. At a given lift coefficient the elevator angle required for a given shift in c.g. can be determined. The evaluation of elevator power can be made according to the above equation. The results of this method of determining elevator power are shown plotted on Figure 17 being labeled "approximate equation".

The above method is only approximate since no correction was made for the change in airplane lift caused by the elevator. The second method corrected $C_{m_{\delta_e}}$ for the lift due to the elevator. To explain this effect consider an airplane flying in equilibrium at a given airplane lift coefficient. The total lift represented by the lift coefficient is the sum of the contribution of the wing and tail equalling the weight of the airplane. If the center of gravity is moved aft and the same airplane lift is to be maintained, the wing lift must decrease by the amount that the tail lift increases to maintain an equilibrium of pitching moments. The wing lift will be decreased by changing the wing angle of attack with the elevator. At the same lift, the distribution of the lift between the wing and tail will be changed; therefore, the assumption, that at a constant airplane lift coefficient the wing lift coefficient will also be constant for an c.g. movement, is incorrect.

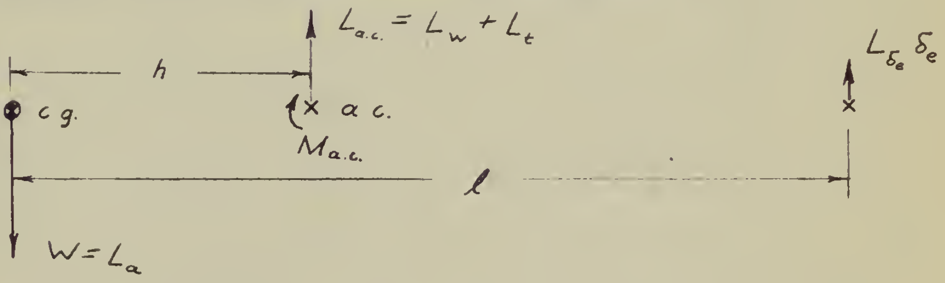

$$\Sigma F_z = L_{a.c.} + L_{\delta_e}\delta_e - L_a = 0$$

$$\Sigma M_{c.g.} = M_{a.c.} - h L_{a.c.} - \ell L_{\delta_e}\delta_e = 0$$

$$M_{a.c.} - hL_a - (l-h)L_{\delta_e}\delta_e = 0$$

For small changes

$$(1) \quad -L_a - (l-h)L_{\delta_e}\frac{d\delta_e}{dh} = 0$$

$$(2) \quad -h - (l-h)L_{\delta_e}\frac{d\delta_e}{dL_a} = 0$$

Combining (1) and (2)

$$\frac{h}{c} = \frac{L_a}{\frac{d\delta_e}{dh/c}} \cdot \frac{d\delta_e}{dL_a} = C_{L_a}\frac{\frac{d\delta_e}{dC_{L_a}}}{\frac{d\delta_e}{dh/c}} = -\frac{dC_m}{dC_L}$$

By substituting "h" into (1)

$$\frac{1}{L_{\delta_e}} = -\frac{l}{L_a}\frac{d\delta_e}{dh} + \frac{d\delta_e}{dL_a}$$

$$\frac{1}{C_{m_{\delta_e}}} = \frac{\frac{d\delta_e}{dh/c}}{C_{L_a}} - \frac{\frac{d\delta_e}{dC_{L_a}}}{l/c}$$

To determine the corrected elevator power the slope $\frac{d\delta_e}{dC_{L_a}}$ was measured at various lift coefficients for each c.g. curve. To determine the slope $\frac{d\delta_e}{dh/c}$, the neutral points were obtained from Figure 13, which is a plot of $\frac{d\delta_e}{dC_{L_a}}$ versus x_{cg}/c. Since h/c is the difference between the neutral point and the c.g. position, Figure 14 gives the desired $\frac{d\delta_e}{dh/c}$. The corrected values of elevator power for the three c.g. positions are

shown plotted on Figure 17. They are larger than the approximate method results since disregarding this lift change gives an underestimated value for $C_{m_{\delta_e}}$. The increment between the constant c.g. curves was caused by the changes in tail length. This is proven by comparing the per cent of change in elevator power with the per cent in tail length. Elevator power is directly proportional to tail length.

A third method of determing C_{m_δ} , with tail lift effect considered, was devised to determine the extent of any non-linearities of elevator due to pitching velocity, $d\theta$, and c.g. changes. In order to make the evaluation a plot of C_{La} - x_{cg}/c - $d\theta$ versus δ_e was established. The pitching velocity is defined in operator form in accordance with Reference 1 as

$$d\theta = \tfrac{1}{2}C_{La} \ (1 - 1/n^2).$$

The values of δ_e versus V_e , as shown in Figures 1, 2 and 3, were plotted in terms of δ_e versus C_{La} as shown in Figures 10, 11 and 12. Taking data directly from the latter curves gave a very limited range of usable data. This difficulty was avoided by making a plot of δ_e versus $d\theta$ for c.g. positions as shown in Figure 15. By taking a cross-plot from Figure 15 and making the necessary calculations, the curves of C_{La} - x_{cg}/c - $d\theta$ versus δ_e for $d\theta$ = 0, 0.1 and 0.2 were plotted on Figure 16. An auxiliary plot of $d\theta$ = 0.05 and 0.15 was used to establish more data, but was not included in this report. Values of $\frac{d\delta_e}{d\,h/c}$ and $\frac{d\delta_e}{dC_{L_a}}$ were measured, as illustrated by Figure 16, for constant values of lift coefficient, pitching velocity and c.g. position. The slope $\frac{d\delta_e}{d\,h/c}$ was constant for each lift coefficient and $\frac{d\delta_e}{dC_{L_a}}$ is part of a small corrective term which varied slightly

with center of gravity location. Therefore, the evaluated elevator power was plotted for only one c.g. position, $x_{cg}/c = 0.368$. The elevator power versus lift coefficient curves for constant pitching velocity is shown plotted on Figure 18.

When the $d\theta = 0$ curve of Figure 18 is compared with the curve for the same c.g. of Figure 17, it is noted that at high lift coefficients there is a marked discrepancy. It is believed that the curves of Figure 18 are the more representative in this range since the data used in computing the curves of Figure 17 was limited in this region. No attempt was made to replot the data in another form to extend its useful range. Other than as noted above, the comparison of values is reasonable in the light of the fact that slopes were multiplied during the computations.

The analytical computation for elevator power was determined in accordance with Reference 2.

$$\begin{aligned} C_{m_\delta} &= -a_t \bar{V} \eta_t \tau_e \\ &= -(.052)(.717)(1)(.6) \\ &= -.0224 \ / \ deg \end{aligned}$$

The analytical value is plotted on Figure 17 for a mean c.g. location. This value compares to within less than two per cent of a corrected C_{m_δ} for a comparable position and speed. If account could be made for the change of tail efficiency with a variation in lift coefficient, it is expected that the analytical value for elevator power would give close correlation at the other lift coefficients.

With a fixed pitch propeller it is impossible to maintain constant power over the speed range investigated. At a low lift coefficients

the propeller RPM increased and at high lift coefficients it dropped off. This variation of RPM obviously affected the tail efficiency causing a variation of elevator power with lift coefficient.

Considering the variation of elevator power with pitching velocity, as shown in Figures 18 and 21, it is observed that elevator power increases as the airplane's pitching velocity increases to $d\theta = 0.05$. As the pitching velocity is further increased the elevator power gradually decreases until at $d\theta = 0.2$ the value is less than at $d\theta = 0$. This particular variation of elevator power indicates that the tail has gone through the slipstream center. The increased variation at high lift coefficients validates this reasoning. In accordance with Reference 1, this slipstream and wake effect is due to the changes in downwash and tail efficiency with pitching velocity and lift coefficient. Further investigation would be necessary to determine the respective effects of tail efficiency and downwash with a variation of pitching velocity.

The stick fixed trim curves are among the most accurate data that may be obtained from flight testing an airplane. The pilot technique is relatively simple and the accuracy depends primarily on how accurate the elevator angle and airspeed can be measured. Accurate instrumentation is, therefore, a necessity. The use of this data to evaluate the elevator power produces results that are in good agreement with theory. The second method to obtain the elevator power is the most accurate. This method corrected for the tail lift, which is a refinement of the first approximate method. The third method is liable to errors since three slopes were used in the calculation. This particular evaluation, however, is an aid to determine the variation of elevator power with the parameter $d\theta$.

$C_{md\theta}$:

An airplane in a straight, unaccelerated flight path is in equilibrium at a particular trim lift coefficient. That is, at each trim point, the lift is equal to the weight and the condition that C_LV^2 equals a constant is maintained. As the airplane speed is increased or decreased, the lift will change accordingly and require the elevator to maintain the equilibrium situation. The unaccelerated flight equilibrium of pitching moments is

$$C_{m_{c.g.}} = C_{m_o} + \left(\frac{dC_m}{dC_L}\right)_{C_LV^2=K} \Delta C_L + C_{m_\delta} \Delta \delta_e .$$

If the airplane is placed in a steady turn, the lift must increase to provide a vertical component equal to the weight. This increase of lift taken place with no change of speed, and the elevator needed for equilibrium of pitching moments is different than the change of lift for the constant C_LV^2 case. This difference occurs, since the lift is increased with the speed being constant in the steady turn; therefore, the curved flight path will produce a rotation of the airplane about its Y-axis with the introduction of a damping moment. This damping moment is opposed by the elevator lift increment. The magnitude of the damping moment can be estimated since this elevator change can be separated from the elevator needed for unaccelerated flight. (See Figures 10, 11 and 12)

If the damping derivative is expressed in the coefficient form $C_{md\theta}$, the equilibrium of pitching moments for accelerated flight is

$$C_{m_{c.g.}} = C_{m_0} + \left(\frac{dC_m}{dC_L}\right)_{V=K} \Delta C_L + C_{m_{d\theta}} d\theta + C_{m_\delta} \Delta \delta_e$$

With the airplane lift coefficient defined as

$$C_{La} = \frac{2n\ W/S}{\rho V^2}$$

the lift coefficient for the accelerated flight will be greater than the unaccelerated flight by the amount of "g" at a given speed. Figures 10, 11 and 12 are elevator angle versus airplane lift coefficient curves taken from the elevator angle versus equivalent velocity curves for the steady turns. The increment of elevator angle between the 1-g and any of the accelerated flight curves for a particular c.g. location will be that increment of elevator angle required to overcome the damping in pitch of the airplane. If no damping moments existed the curves of elevator angle versus lift coefficient would coincide for the various g's since a given elevator angle would produce the same lift at any acceleration. This assumes that the airplane's static stability does not vary with the different slipstream characteristics encountered in obtaining the data.

If stability variations are neglected, then at any lift coefficient the equilibrium condition is given by

$$C_{m_{d\theta}} + C_{m_\delta} \Delta \delta_e = 0$$

$$C_{m_{d\theta}} = - \frac{C_{m_\delta} \Delta \delta_e}{d\theta}$$

$$d\theta = \frac{1}{2} C_{L_a} \left(1 - \frac{1}{n^2}\right)$$

(d) is the operator $\frac{d}{d(t/\tau)}$.

The damping derivative was determined by the above method and the results are plotted for a variation of lift coefficient in Figure 19. As the damping in pitch is normally not a function of lift coefficient, an average experimental value of damping in pitch can be obtained. The variation of this derivative can be attributed to the assumption that the variation of the airplane's static stick fixed longitudinal stability for accelerated and unaccelerated flight under the two slipstream conditions of C_LV^2 equal a constant and V equal a constant is negligible.

The analytical computation for damping in pitch was evaluated in accordance with Reference 2. The total damping in pitch of an airplane is the sum of the damping contributions of the various airplane components. In the normal configured airplane the damping due to the tail is by far the largest factor. This damping occurs as a direct result of the change in the effective angle of attack of the tail produced by the pitching velocity of the airplane. The change in tail angle of attack is given by $\Delta\alpha_t = \dot{\theta}\frac{l_t}{V}$. The pitching moment produced by this angle of attack is

$$C_m = -a_t \eta_t \bar{V} \frac{d\theta}{dt} \frac{l_t}{V},$$

for which

$$C_{m_{d\theta}} = -a_t \eta_t \bar{V} \frac{l_t}{c} \frac{1}{\mu}$$

$$= -\frac{(.052)(.717)(1)(14.1)(57.3)}{(4.75)(40)}$$

$$= -.183/\text{radian}.$$

This theoretically determined value is plotted on Figure 19 to facilitate comparison with the experimental curves. This discrepancy between the experimental and theoretical results may be due to one or more factors. The errors in the elevator power have been carried along in the damping in pitch determination.

Another important factor is the assumption that the airplane's static stick fixed longitudinal stability remained constant during these tests. It was assumed that the change in elevator angle required in accelerated flight at a particular lift coefficient was due to the damping in pitch of the airplane. From Reference 1 it can be shown that

$$\frac{d\delta_e}{dC_{L_a}} = - \frac{dC_m/dC_{L_a}}{C_{m_\delta}} .$$

If there is any variation of $\frac{dC_m}{dC_L}$, the previous method of determing the damping in pitch is in error. An attempt was made to investigate this effect of stability variation by determining the neutral point for various pitching velocities and lift coefficients. This was done by use of the previously developed formula

$$\frac{h}{c} = C_{L_a} \frac{\frac{d\delta_e}{dC_{L_a}}}{\frac{d\delta_e}{dh/c}} = N_o - x_{c.g.} .$$

These neutral points were determined by use of Figure 16. The resulting neutral points are shown plotted on Figures 23 and 24. The results show an increase of static stability as the pitching velocity increases;

therefore, the damping derivative determined by the steady state technique is high due to this increase of static stability. $C_{md\theta}$ does not vary with static stability, but the process of evaluation introduces errors caused by this variation of static stability.

A third source of error which may account for part of the discrepancy between the theoretical and experimental results lies in the theoretical calculation itself. The theoretical evaluation considered only the tail contribution. No consideration was made for the damping contribution of the fuselage, wing and propeller. These damping contributions are very difficult to determine and are usually accounted for by use of a multiplying factor in the tail damping computation. Reference 2 suggests that this multiplier be 1.1. Some authoritative sources in the airplane stability field believe that it should be higher. It is probably merely an "educated guess" for the value of this factor.

Another experimental evaluation of the damping in pitch was made by measuring the slope of $\frac{d\delta_e}{d\theta}$ from Figure 16 for the value of the $\frac{\Delta\delta_e}{d\theta}$ factor. The elevator power value was for a particular $C_{L\alpha}$, x_{cg}/c and $d\theta$. The resultant damping in pitch coefficient is shown plotted on Figure 21 for the x_{cg}/c = 0.368 data. These curves had the same order of arrangement with respect to pitching velocity as the elevator power curves. The $C_{md\theta}$ curve from Figure 19 for the same c.g. position was plotted on Figure 20 to make a comparison of the results of the two methods. Since the acceleration was 1.8g for this curve, the value of pitching velocity varied with lift coefficient. The values of pitching velocity are shown on Figure 20 for this curve. These values are in their proper relative position with respect to the other curves at constant pitching

velocity except for $C_{La} = 0.7$. This divergence is an end point evaluation and could be expected.

The variation of the damping in pitch coefficient with pitching velocity is shown plotted in Figure 22 for three lift coefficients. From these curves it is obvious that damping in pitch has little change with pitching velocity at a constant lift coefficient. Since Figure 22 shows that there is slight variation of the $C_{md\dot{\theta}}$ with pitching velocity and Figure 20 shows that the c.g. location has little effect, it follows that the variation of $C_{md\dot{\theta}}$ evaluated in this manner must be due to the static stability variations of accelerated and unaccelerated flight.

The flight test technique for evaluating the airplane's damping in pitch has been outlined and discussed. The criterion is whether or not the method produces results of sufficient accuracy to be practical. The pilot technique consists of measuring the airspeed, acceleration and elevator deflection with the airplane in a steady banked turn at a constant airspeed. These variables can be measured with considerable accuracy with proper instrumentation. If the elevator power is accurately known, it should be possible to reduce the flight data to a fairly accurate value of $C_{md\dot{\theta}}$. The major source of error is the determination of elevator power as discussed previously. Another source of error is the static stability variation introduced by accelerated flight with propeller driven airplanes.

The difficulties encountered in separating the variables and accounting for the errors do not rule out this technique for obtaining the damping

velocity except for $C_{La} = 0.7$. This divergence is an end point evaluation and could be expected.

The variation of the damping in pitch coefficient with pitching velocity is shown plotted in Figure 22 for three lift coefficients. From these curves it is obvious that damping in pitch has little change with pitching velocity at a constant lift coefficient. Since Figure 22 shows that there is slight variation of the $C_{md\dot{\theta}}$ with pitching velocity and Figure 20 shows that the c.g. location has little effect, it follows that the variation of $C_{md\dot{\theta}}$ evaluated in this manner must be due to the static stability variations of accelerated and unaccelerated flight.

The flight test technique for evaluating the airplane's damping in pitch has been outlined and discussed. The criterion is whether or not the method produces results of sufficient accuracy to be practical. The pilot technique consists of measuring the airspeed, acceleration and elevator deflection with the airplane in a steady banked turn at a constant airspeed. These variables can be measured with considerable accuracy with proper instrumentation. If the elevator power is accurately known, it should be possible to reduce the flight data to a fairly accurate value of $C_{md\dot{\theta}}$. The major source of error is the determination of elevator power as discussed previously. Another source of error is the static stability variation introduced by accelerated flight with propeller driven airplanes.

The difficulties encountered in separating the variables and accounting for the errors do not rule out this technique for obtaining the damping

in pitch of the airplane. The technique requires less reduction of data and instrumentation than the frequency response method. It is believed that with good pilot technique, dependable instrumentation and the elimination of as many of the variables as possible, the steady state flight testing to determine the damping in pitch derivative is the most accurate method for subsonic aircraft.

Lateral

The equations for steady state lateral motion, as developed in Reference 1 and 2, are written below with secondary control actions included.

$$(1)\quad C_{y_\beta}\beta - C_L \frac{V}{g}\dot{\psi} + C_L \phi + C_{y_{\delta_r}}\delta_r = 0$$

$$(2)\quad C_{l_\beta}\beta + C_{l_r}\frac{b}{2V}\dot{\psi} + C_{l_{\delta_a}}\delta_a + C_{l_{\delta_r}}\delta_r = 0$$

$$(3)\quad C_{n_\beta}\beta + C_{n_r}\frac{b}{2V}\psi + C_{n_{\delta_a}}\delta_a + C_{n_{\delta_r}}\delta_r = 0$$

These equations are the side force, rolling moment and yawing moment equations of motion for an airplane in a steady lateral maneuver. Since the equations consist of five variables, it was necessary to eliminate certain of the unknowns in order to determine the derivatives. The use of two flight techniques reduces the number of variables to four in each case. The straight sideslip maneuver was performed with $\dot{\psi} = 0$; the skidding turn was performed with $\phi = 0$. As there are three equations, solutions for the derivatives can be obtained as ratios of the control forces or moments involved.

To find a solution for the derivatives, the primary control moments were measured directly. The rudder control power, $C_{n_{\delta_r}}$, was determined by introducing a known yawing moment about the Z-axis and measuring the change in the rudder angle needed to balance the moment. This derivative was obtained by use of the steady sideslip technique with the airplane both "clean" and with the towed drogue. The equation of equilibrium for this situation is

$$C_{n_\beta}\beta + C_{n_{\delta_r}}\delta_r + C_{n_{\delta_a}}\delta_a + C_{n_o} = 0$$

$$C_{n_o} = \frac{D_t\, y}{q\, S\, b}$$

D_t = Drag of drogue

y = Distance of drogue attachment to Z-axis.

The rudder angle needed to balance the yawing moment introduces a rolling moment. A small aileron angle is needed to restore the equilibrium in roll. This slight angle is multiplied by a secondary effect and can be neglected. The rudder increment measured at $\beta = 0$ for the two runs is determined from Figures 4 and 5. The value for $C_{n_{\delta_r}}$ is

$$C_{n_{\delta_r}} = -\frac{D_t\, y}{q\, S\, b\, \delta_r}$$

$$= -\frac{(41)(9.075)}{(25.6)(155)(33.965)(1.9)}$$

$$= -.00146 \,/\, \text{degree}$$

$$= -.0835 \,/\, \text{radian.}$$

An analytical determination was made for rudder power in accordance with Reference 2:

$$C_{n_{\delta_r}} = -a_v \tau \frac{S_v l_v}{S_w b} \eta_t$$

$$= -\frac{(.052)(.6)(14.1)(16.75)}{(34)(155)} (1)$$

$$= -.0016 / \text{degree}$$

$$= -.0916 / \text{radian}$$

It is observed that the flight test and analytical evaluations of rudder power are in a very close agreement.

The lateral control power, $C_{l_{\delta_a}}$, was determined by use of a known rolling moment about the X-axis and measuring the change of aileron angle used to restore equilibrium. These steady sideslip technique tests were made with the airplane both "clean" and with the wing weight added. The equation for equilibrium for this maneuver is

$$C_{l_\beta} \beta + C_{l_{\delta_a}} \delta_a + C_{l_{\delta_r}} \delta_r + C_{l_a} = 0$$

C_{l_a} = $W_a\, y/qSb$

W_a = added weight

y = distance of weight from X-axis

The above noted change of aileron angle will introduce a yawing moment due to adverse yaw, consequently, a change of rudder angle. This is normally a small angle which is multiplied by a secondary control effect;

therefore, the $C_{l_{\delta_r}}$ term is dropped. Thus, taking the aileron increment at $\beta = 0$ for the two runs of Figures 4 and 6, the value for lateral control power becomes

$$\begin{aligned} C_{l_{\delta_a}} &= -\frac{W_a\, y}{q S b \delta_a} \\ &= -(29)(9.05)/(25.6)(155)(33.965)(-1.7) \\ &= +.001145/\text{degree} \\ &= +.0656/\text{radian.} \end{aligned}$$

An analytical determination was made for lateral power in accordance with Reference 2:

$$\begin{aligned} C_{l_{\delta_a}} &= \frac{a_w \tau}{S_w b}\int_{k_1 \frac{b}{2}}^{k_2 \frac{b}{2}} c y \, dy \\ &= \frac{(1)(.08)(.5)}{(155)(34)}\int_{8.33}^{14.33} 4.75 \, y \, dy \\ &= .00246/\text{degree} \\ &= .141/\text{radian} \end{aligned}$$

By use of charts for estimating $C_{l_{\delta_a}}$ from NACA TR 635, this value was found to be .1065. It is observed that the flight test and analytical evaluations of lateral control power are not in good agreement. The analytical value is somewhat high because of errors due to the strip integration process used. A possible error involved in the flight test value is the disregard of adverse yaw effect.

An investigation was made to determine the effects of the secondary control moments and the effect of the slight rolling moment introduced

by the drogue. The following equations of motion are written with the subscript (1) for the drogue effect and the subscript (2) for the wing weight effect:

$$\text{(a)}\quad \Delta\delta_{r_1} C_{n_{\delta_r}} + \Delta\delta_{a_1} C_{n_{\delta_a}} = -(\Delta C_n)_1$$

$$\text{(b)}\quad \Delta\delta_{r_1} C_{l_{\delta_r}} + \Delta\delta_{a_1} C_{l_{\delta_a}} = -(\Delta C_l)_1$$

$$\text{(c)}\quad \Delta\delta_{r_2} C_{n_{\delta_r}} + \Delta\delta_{a_2} C_{n_{\delta_a}} = 0$$

$$\text{(d)}\quad \Delta\delta_{r_2} C_{l_{\delta_r}} + \Delta\delta_{a_2} C_{l_{\delta_a}} = -(\Delta C_l)_2$$

From Figures 4 and 6 it is seen that no change of rudder occurred, measured at $\beta = 0$; therefore, from equation (c) the secondary control effect, $C_{n_{\delta_a}}$, is zero. It is believed that with a larger wing weight some value of adverse yaw might have been obtained. From equations (a) and (d) it is observed that rudder and aileron power are as calculated previously. Equation (b) is used to evaluate the secondary control moment due to rudder angle, $C_{l_{\delta_r}}$. The increments of δ_{a_1} and δ_{r_1} are taken from Figures 4 and 5. The rolling moment caused by the drogue was determined by estimating the angle of the tow line at the lift strut to the horizontal reference. Thus, the vertical component of the drogue force was established. To this force was added the weight of the fittings on the lift strut. Therefore, $C_{l_{\delta_r}}$ becomes

$$C_{l_{\delta_r}} = -\frac{(\Delta C_l)_1}{\Delta\delta_{r_1}} - \frac{\Delta\delta_{a_1}}{\Delta\delta_{r_1}} C_{l_{\delta_a}}$$

$$= -\frac{.000402}{1.9} - \frac{-.7}{1.9}(.001145)$$

$$= .000211 \ / \ \text{degree}$$

$$= .0121 \ / \ \text{radian}$$

Another evaluation of $C_{l_{\delta_r}}$ was made by considering the following geometric relationship:

$$C_{l_{\delta_r}} = - C_{n_{\delta_r}} \frac{h_v}{l_t} = -(-.00146)\frac{(2.1)}{(13.6)}$$

$$= +.000226 \,/\, degree$$

$$= +.0130 \,/\, radian$$

The results of the two methods of determing $C_{l_{\delta_r}}$ are in good agreement.

Using a geometric relationship in a similar manner, the secondary side force derivative can be determined as follows:

$$C_{y_{\delta_r}} = - C_{n_{\delta_r}} \frac{b}{l_t} = -(-.00146)\frac{(33.965)}{13.6}$$

$$= +.00364 / \, degree$$

$$= +.209 \,/\, radian$$

The side force derivative, C_{y_β}, was obtained from the flight test curves which showed the variation of angle of bank and rudder angle with straight sideslip, Figure 4. Thus equation (1) becomes

$$C_{y_\beta} = - C_L \frac{d\phi}{d\beta} - C_{y_{\delta_r}} \frac{d\delta_r}{d\beta}$$

$$= -(.562)(.71) - (.232)(.4)$$

$$= -.398 \quad -.093$$

$$= -.4909 \,/\, radian.$$

By comparison with the magnitudes of other derivatives it is seen that this derivative is very important.

The dihedral effect of this airplane was determined from the straight sideslip manouver with the airplane "clean", Figure 4. Thus equation (2) becomes

$$C_{\ell_\beta} = -C_{\ell_{\delta_a}} \frac{d\delta_a}{d\beta} - C_{\ell_{\delta_r}} \frac{d\delta_r}{d\beta}$$

$$= -(.0656)(.76) - (.0144)(.4)$$

$$= -.05656 / \text{radian}.$$

The analytical determination of dihedral effect, in accordance with Reference 2, is

$$C_{\ell_\beta} = (C_{\ell_\beta})_{wing} + (C_{\ell_\beta})_{v.tail} + (\Delta C_{\ell_\beta})_1 + (\Delta C_{\ell_\beta})_2$$

$$= -.000808 - .000382 - .00060 + .00016$$

$$= -.001628 / \text{degree}$$

$$= -.0933 / \text{radian}$$

The flight test and analytical values of C_{l_β} are in fair agreement. The analytical evaluation contains approximations which make this result merely a good estimate. The flight test value might be low since $C_{l_{\delta_a}}$ is believed to be too small. The airplane does have stable dihedral effect.

When the longitudinal axis of the airplane is yawed from the relative wind, a yawing moment is created about the Z-axis. This weather-cocking is referred to as directional stability, C_{n_β} . The directional

stability of this airplane can be determined by use of the straight sideslip test data, Figure 4. Thus equation (3) becomes

$$C_{n_\beta} = -C_{n_{\delta_r}} \frac{d\delta_r}{d\beta} - C_{n_{\delta_a}} \frac{d\delta_a}{d\beta}$$

$$= -(-.0835)(.4) - (0)$$

$$= +.0334 / \text{radian.}$$

The analytical determination of C_{n_β}, in accordance with Reference 2, is

$$C_{n_\beta} = (C_{n_\beta})_{wing} + (C_{n_\beta})_{Fuse.} + (C_{n_\beta})_{prop} + (C_{n_\beta})_{v.tail} + \Delta_1 C_{n_\beta} + \Delta$$

$$= 0 + (-.0012) + (-.000127) + (.00267) + (.0002) +$$

$$= .000943 / \text{degree}$$

$$= .054 / \text{radian.}$$

The analytical and flight test values agreed better than was expected, since the analytical derivatives contained estimates and the fuselage contribution was an empirical determination. The flight test result might possibly be greater, since $C_{n_{\delta_a}}$ could have a very small value rather than zero as found in this investigation. The airplane does have directional stability.

Damping in yaw, C_{n_r}, is similar to $C_{m_{\dot\theta}}$ in that most of the damping is due to the increase in angle of attack of the vertical tail as the airplane is yawed. Evaluation of this derivative is possible by using a combination of the straight sideslip and skidding turn equations.

If the derivative of equation (3), with respect to sideslip, is taken for the two flight techniques and one subtracted from the other, C_{n_r} is determined as follows:

$$C_{n_r} = \frac{\left[\left(\frac{d\delta_r}{d\beta}\right)_{SS} - \left(\frac{d\delta_r}{d\beta}\right)_{ST}\right]}{\frac{b}{2V} \quad \frac{d\dot{\psi}}{d\beta}} \quad C_{n_{\delta_r}}$$

$$= \frac{\left[(.4) - (.58)\right]}{\frac{33.965}{(2)(147)} \quad (-.525)} \cdot (-.00146)$$

$$= -.00433 / \text{degree}$$

$$= -.248 / \text{radian}$$

The derivative $\left(\frac{d\delta_r}{d\beta}\right)_{SS}$, $\left(\frac{d\delta_r}{d\beta}\right)_{ST}$, and $\frac{d\dot{\psi}}{d\beta}$ are determined from Figures 4, 7 and 8 respectively.

The analytical determination of C_{n_r}, in accordance with Reference 2, is

$$C_{n_r} = -\frac{C_{D_w}}{4} - 2a_v \frac{S_v}{S_w} \left(\frac{l_v}{b}\right)^2 \eta_t$$

$$= -\frac{.0247}{4} - (2)(.06)\frac{(25)}{(155)}\left(\frac{(136)}{(33\ 965)}\right)^2 (1)\ 57.3$$

$$= -.1842 / \text{radian.}$$

The comparison of the flight test and analytical results shows a reasonable agreement. Possible sources of errors of the experimental values is the determinations of the slopes involved. The measurement of $\dot{\psi}$ versus β data was by means of directional gyro compass, and this is liable to some error. However, sufficient flight data was taken to substantiate the results.

The steady state method of determining the lateral stability derivatives yielded results that were reasonable. The pilot technique used to obtain the data was relatively simple. Instrumentation provided accurate measurement of δ_r, δ_a, and β. The bank angle, ϕ, was measured by an attitude gyro, and it is reasonable to expect the gyro to precess at high angles of sideslip and give errors in the reading of ϕ. Visual recording of flight data rather than automatic recording devices also introduced slight errors.

The steady state flight technique produced a very good rudder control power value. This result checked very close with the analytical determination. As an approximate check of $C_{n_{\delta_r}}$, the accepted average value is -.001/ degree in accordance with Reference 2.

Lateral control power, $C_{l_{\delta_a}}$, found by flight test data is possibly too small. The analytical value was much larger than the experimental. The undetected adverse yaw effect might have contributed part of the error. However, the only check for the lateral control power is the analytical determination which is an approximation.

The absence of adverse yaw in the evaluation of the flight data is unusual. A possible reason this was not obtained is that the wing weight might have been too light. With a heavier weight the ailerons would have been deflected more and possibly produced a measureable adverse yaw. Another reason is that $C_{n_{\delta_a}}$ is too small to detect with instrumentation used.

The secondary control moment, $C_{l_{\delta_r}}$, was obtained by two methods of flight data analysis and both are in good agreement. No analytical check was made for $C_{y_{\delta_r}}$ and C_{y_β} but the flight test values are believed to be reasonable. The derivatives C_{n_β} and C_{l_β} have experimental values lower than the analytical determinations. However, both of these analytical calculations contained empirical estimates in addition to approximations for interference factors.

The experimental value of C_{n_r} was compared with an analytical determination that considered only the tail and wing damping in yaw. This comparison showed a reasonable agreement of the two values. A better agreement would result if the damping of the other airplane components were determined analytically. The accuracy of the experimental evaluation depends on how accurate the slopes $\left(\frac{d\delta_r}{d\beta}\right)_{ss}$, $\left(\frac{d\delta_r}{d\beta}\right)_{ST}$, and $\frac{d\dot\psi}{d\beta}$ can be obtained.

CONCLUSIONS

It is concluded as a result of this investigation that accurate longitudinal and lateral stability derivatives can be obtained by the non-oscillatory steady state flight technique. The accuracy of the results is necessarily dependent on the instrumentation and equipment used. However, by use of some improvised instruments and visual recording of data, reasonable, and in some cases excellent results were obtained.

The elevator power, C_{m_δ}, can be determined accurately from the unaccelerated stick fixed trim curves of the Stinson L-5. The assumption that $C_{L_a} = C_{L_w}$ caused only about a 5 per cent error in the values determined for C_{m_δ}. Slipstream effects should be carefully analyzed in order that errors due to variation of the tail efficiency and downwash can be minimized. C_{m_δ} had a variation with pitching velocity due to the tail moving through the slipstream.

The damping in pitch, $C_{m_{d\theta}}$, can be evaluated accurately from the accelerated stick fixed trim curves. The reliability of the $C_{m_{d\theta}}$ evaluation depends upon the accuracy of the C_{m_δ} determined and the accounting for the change of static longitudinal stability for the unaccelerated and accelerated flight conditions. The theoretical determination for $C_{m_{d\theta}}$ should contain a multiplying factor larger than 1.1 as suggested by Reference 2.

The lateral stability derivatives determined for this airplane are as follows:

$C_{n_{\delta_r}} = -.0835/\ \text{radian}$

$C_{l_{\delta_a}} = +.0656/\ \text{radian}$

$C_{l_{\delta_r}} = +.0130/\ \text{radian}$

$C_{y_{\delta_r}} = +.2090/\ \text{radian}$

$C_{y_\beta} = -.4909/\ \text{radian}$

$C_{l_\beta} = -.5656/\ \text{radian}$

$C_{n_\beta} = +.0334/\ \text{radian}$

$C_{n_r} = -.2480/\ \text{radian}$

The flight test lateral derivatives compared favorably with analytical values for this airplane, with the exception of $C_{l_{\delta_a}}$, where the analytical computation is not too reliable.

RECOMMENDATIONS

From the results of this investigation the following recommendations are made:

1. A further study be made of the effects of tail efficiency and downwash on elevator power.

2. A flight test program should be carried out on the Stinson L-5 to determine the variation of static stick fixed longitudinal stability for the $C_L V^2 = K$ and $V = K$ cases in order that the steady state method of evaluating $C_{m_{\delta e}}$ can be corrected for this effect.

3. A further study should be made to determine, for low density airplanes, what portion of the total damping in pitch can be attributed to the propeller, wing, and fuselage.

4. Investigations of this nature inherently involve a certain degree of danger due to engine failure at large angles of sideslip. Suitable modifications should be made to avoid this difficulty.

REFERENCES

1. Perkins, C. D., "Methods For Obtaining Aerodynamic Data Through Steady State Flight Testing", Princeton University Report No. 170.
2. Perkins, C. D. and Hage, R. E., "Airplane Performance Stability and Control", John Wiley and Sons, 1949.
3. Boyd, R. A. and Bothwel, R. L., "Wind Tunnel and Flight Test Investigation of the Cessna 140 for Correlation of Aerodynamic Derivatives", Princeton University Report No. 179.
4. Livingston, W. H., "Determination of the Elevator Power and the Damping in Pitch of the Cessna 140 Airplane From Flight Tests", Princeton University Report No. 160.
5. Graham, D., "Longitudinal Stability and Control Flight Tests of the Cessna 140 Airplane", Princeton University No. 111.
6. Phillips, W. H., "Appreciation and Predication of Flying Qualities", NACA TN 1670, Washington, August 1948.
7. Campbell, J. P. and Mathews, W. O., "Experimental Determination of the Yawing Moment Due to Yawing Contributed by the Wing, Fuselage and Vertical Tail of a Midwing Airplane Model", NACA ARR No. 3F28, Washington, June 1943.
8. Dommasch, D. O., Sherby, S. S. and Connolly, T. F., "Airplane Aerodynamics", Pitman Publishing Co., New York, 1951.

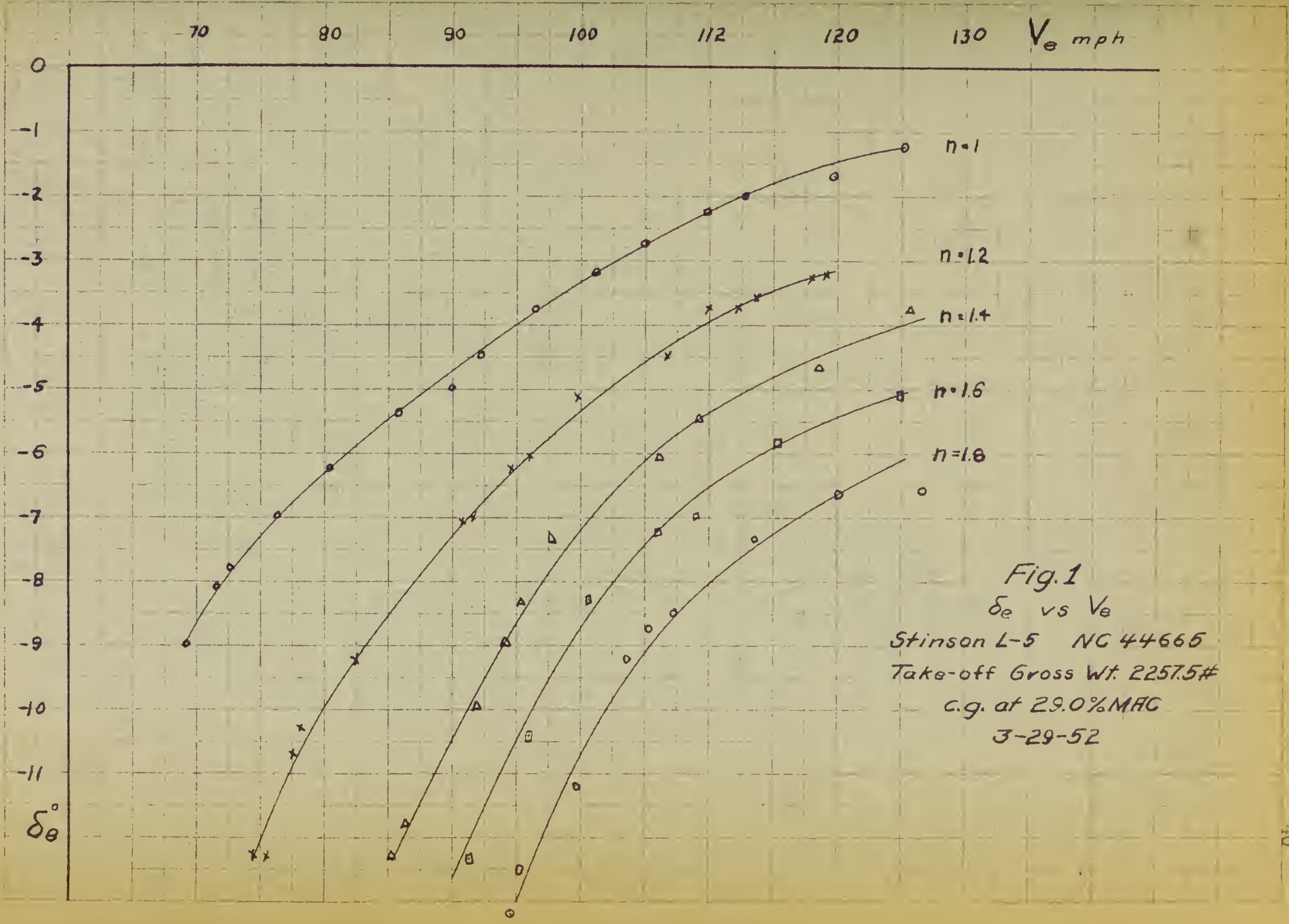

Fig. 1

δ_e vs V_e

Stinson L-5 NC 44665

Take-off Gross Wt. 2257.5#

c.g. at 29.0% MAC

3-29-52

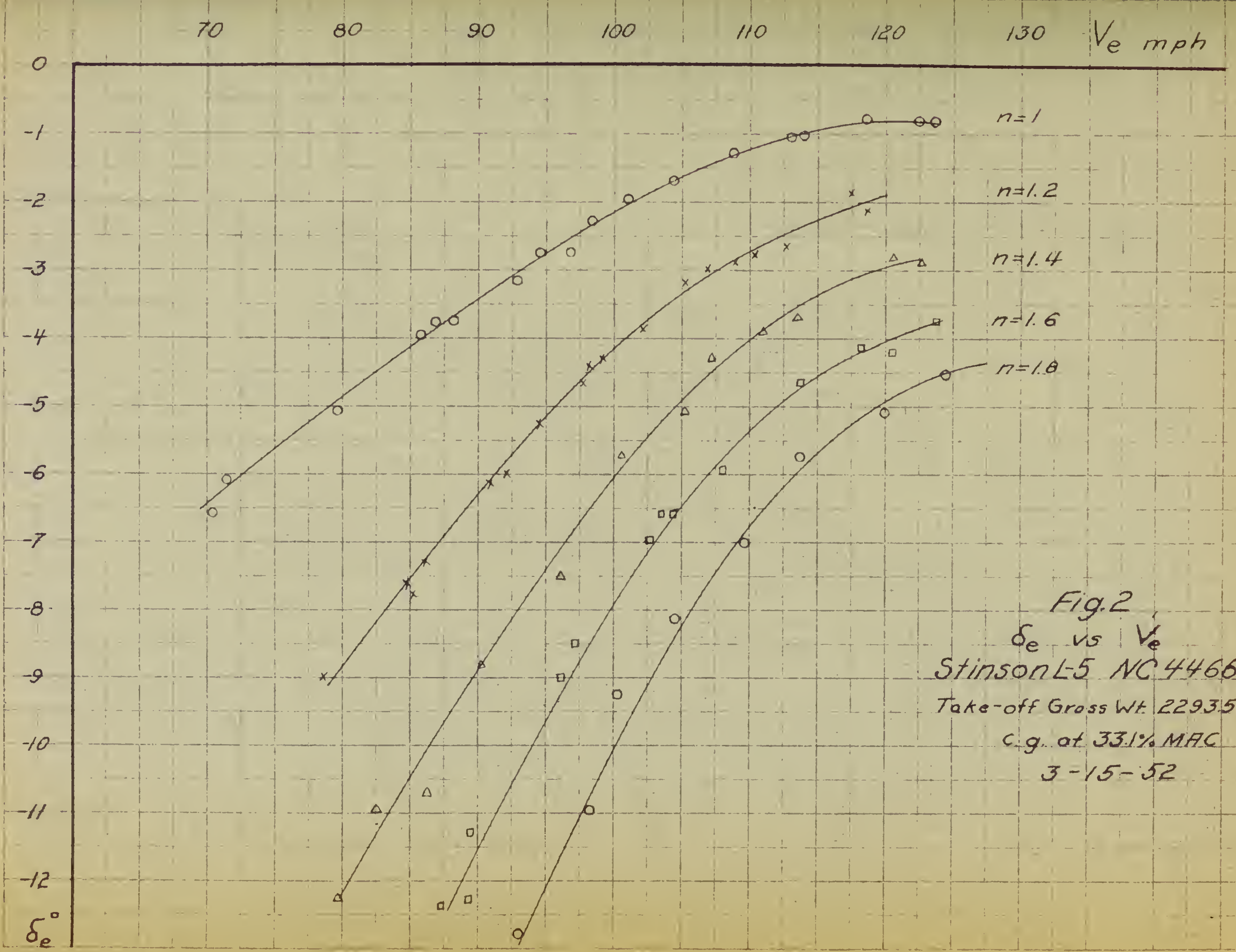

Fig. 2

δ_e vs V_e

Stinson L-5 NC 44665

Take-off Gross Wt. 2293.5#

c.g. at 33.1% MAC

3-15-52

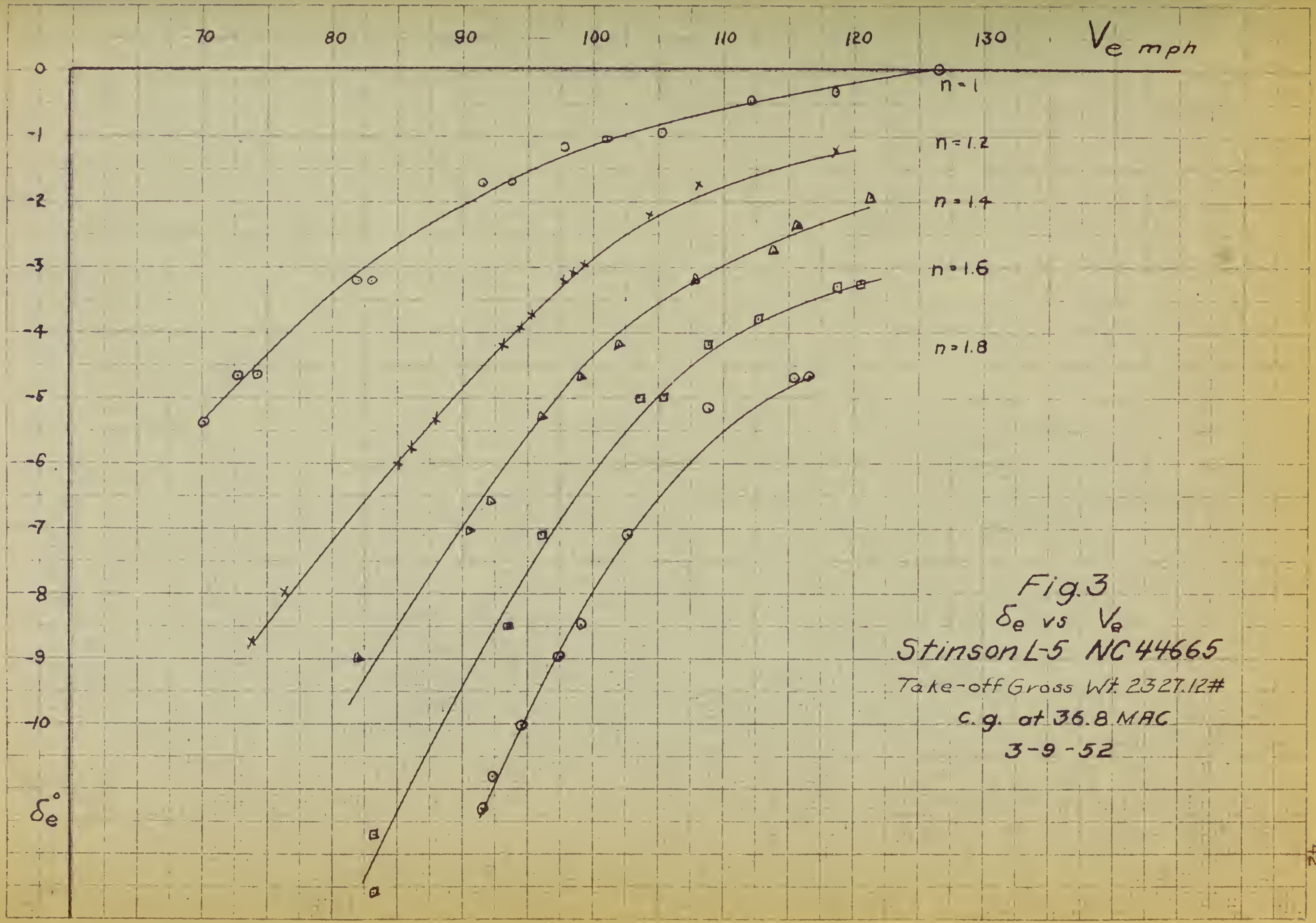

Fig. 3
δ_e vs V_e
Stinson L-5 NC 44665
Take-off Gross Wt. 2327.12#
c.g. at 36.8 MAC
3-9-52

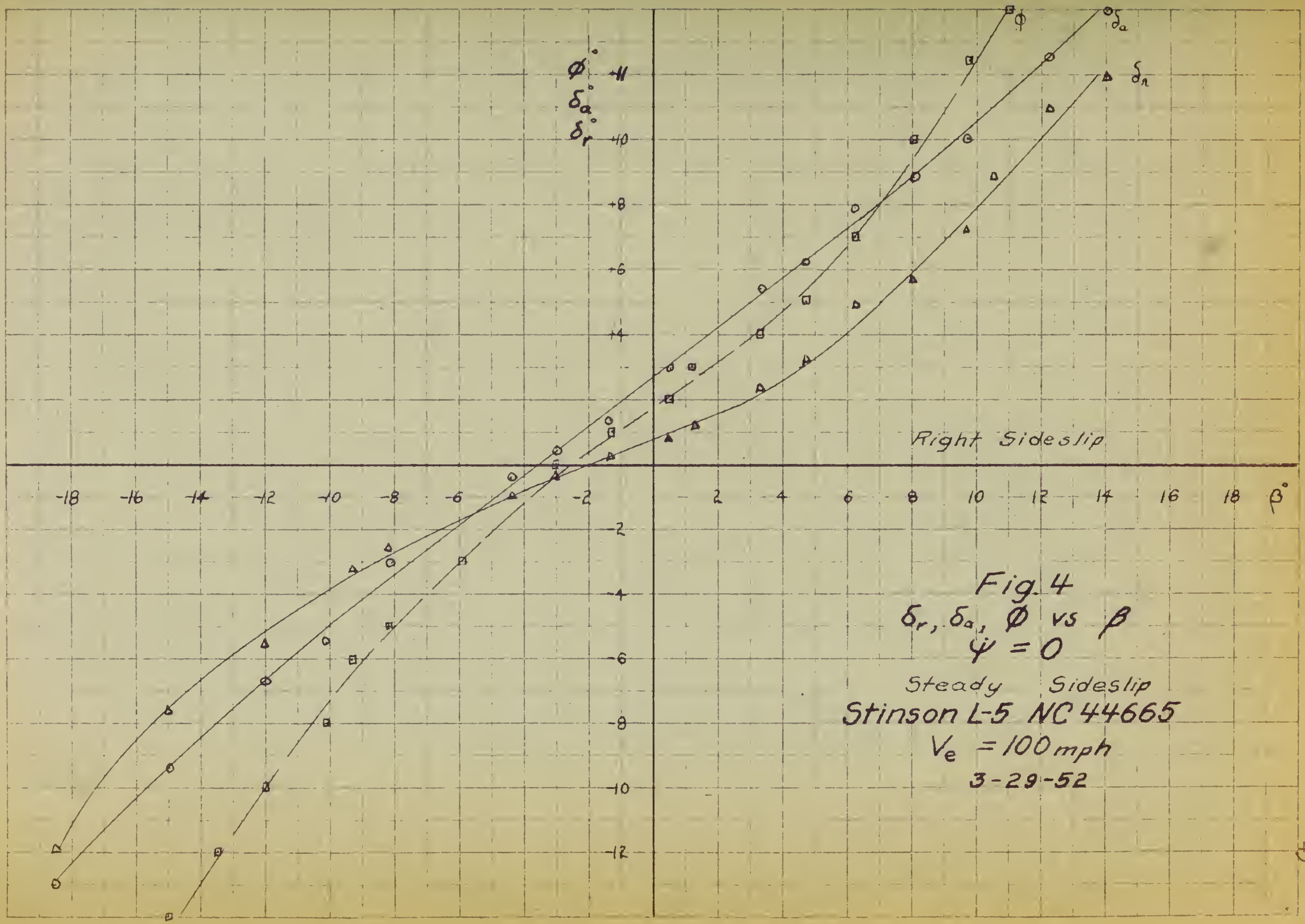

Fig. 4
δ_r, δ_a, ϕ vs β
$\dot{\psi} = 0$
Steady Sideslip
Stinson L-5 NC 44665
$V_e = 100$ mph
3-29-52

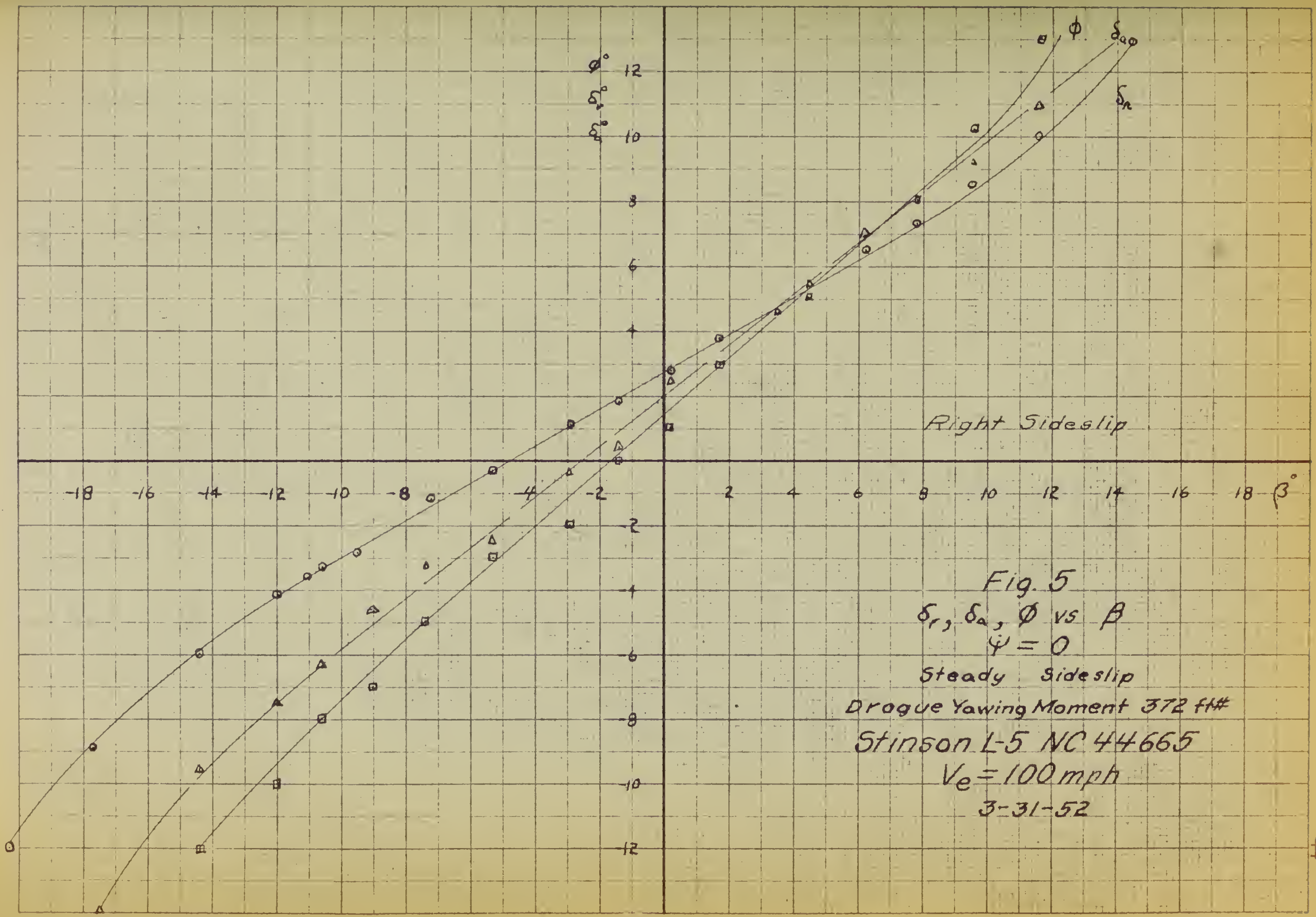

Fig. 5

δ_r, δ_a, ϕ vs β

$\dot{\psi} = 0$

Steady Sideslip

Drogue Yawing Moment 372 ft#

Stinson L-5 NC 44665

$V_e = 100$ mph

3-31-52

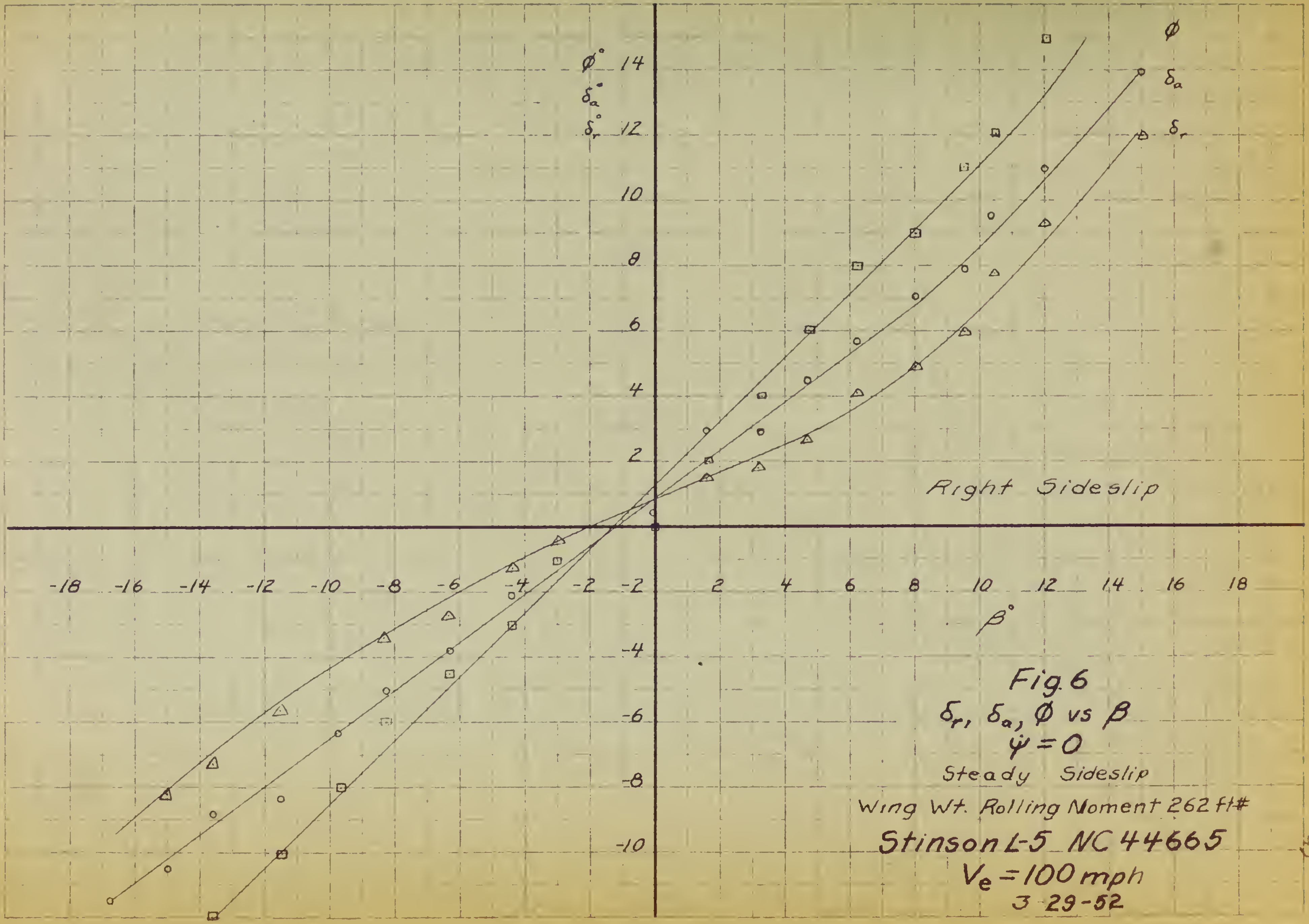

Fig. 6

δ_r, δ_a, ϕ vs β

$\dot{\psi} = 0$

Steady Sideslip

Wing Wt. Rolling Moment 262 ft#

Stinson L-5 NC 44665

$V_e = 100$ mph

3-29-52

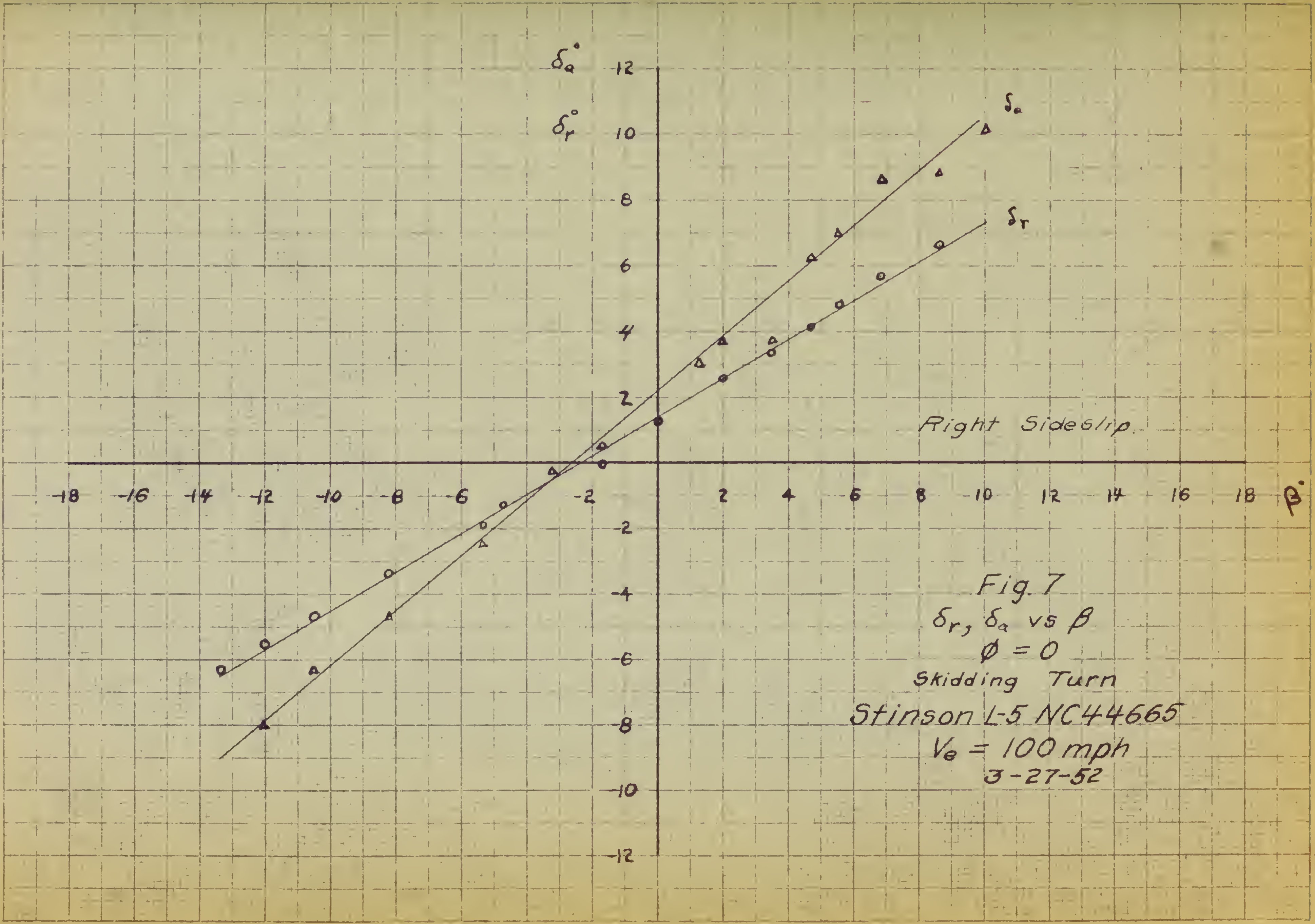

Fig. 7
δ_r, δ_a vs β
$\phi = 0$
Skidding Turn
Stinson L-5 NC44665
$V_e = 100$ mph
3-27-52

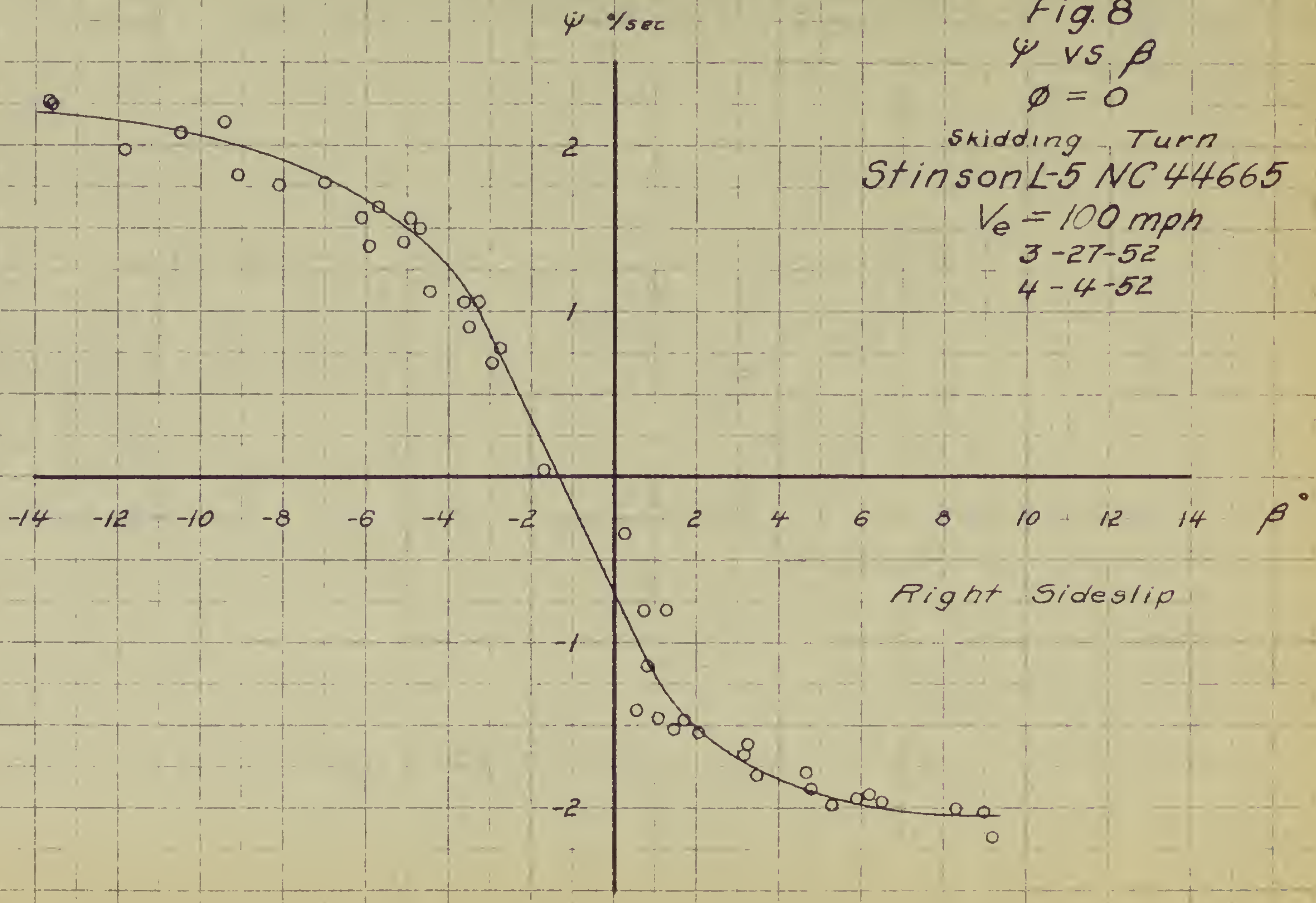

Fig. 8
$\dot{\psi}$ vs. β
$\phi = 0$
Skidding Turn
Stinson L-5 NC 44665
$V_e = 100$ mph
3-27-52
4-4-52

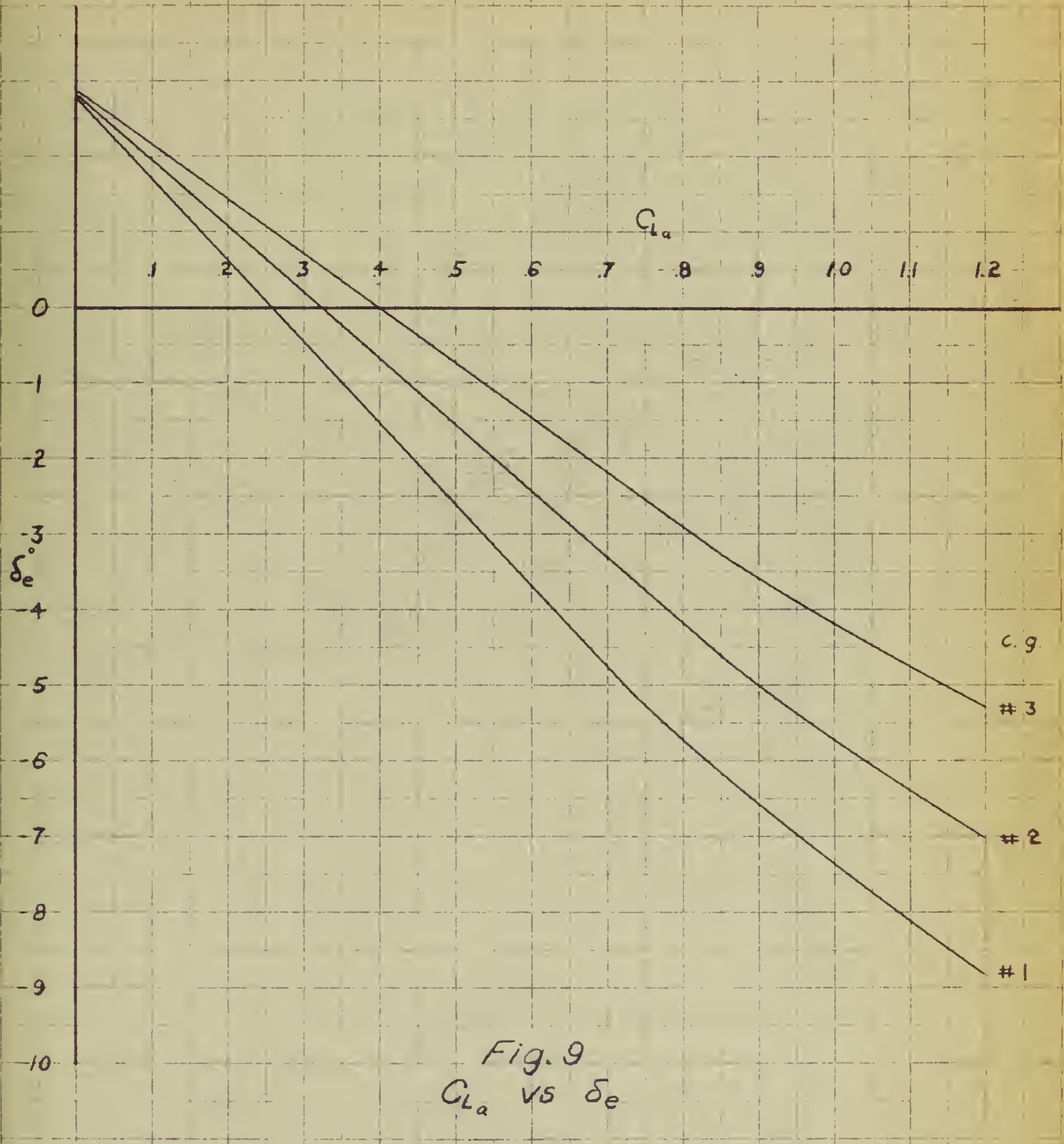

Fig. 9
C_{L_a} vs δ_e

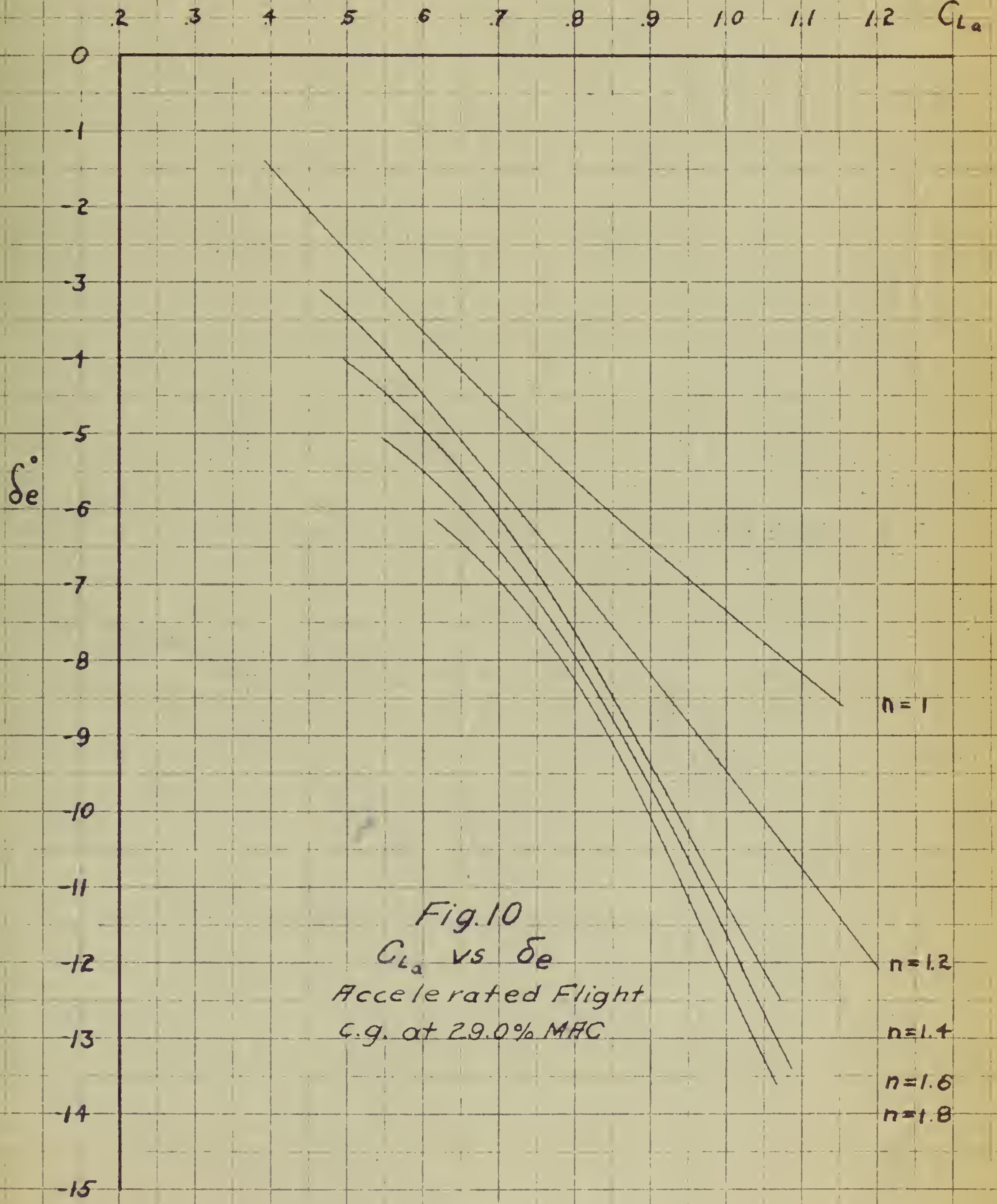

Fig. 10

C_{L_a} vs δ_e

Accelerated Flight

C.g. at 29.0% MAC

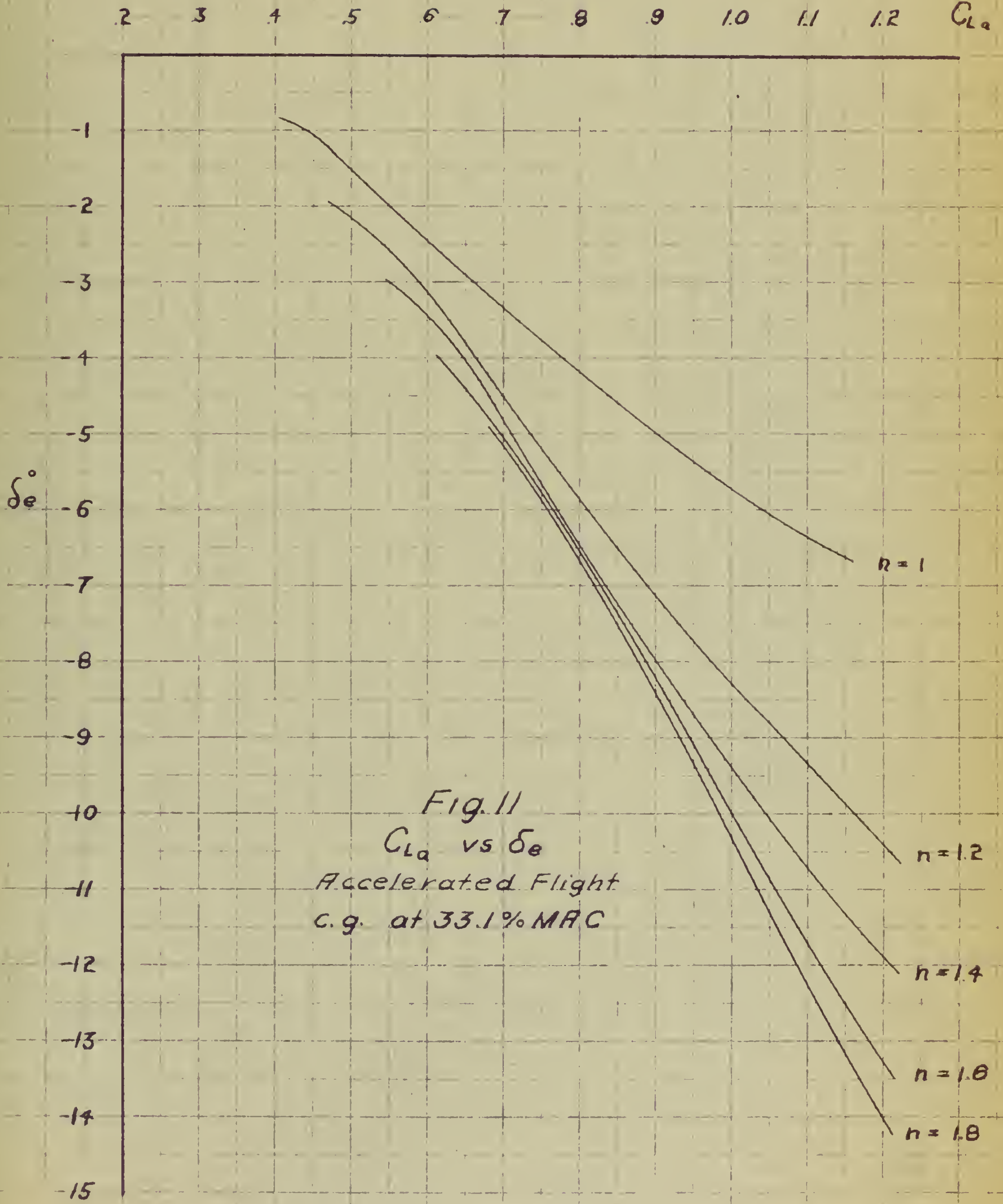

Fig. 11
C_{L_a} vs δ_e
Accelerated Flight
c.g. at 33.1% MAC

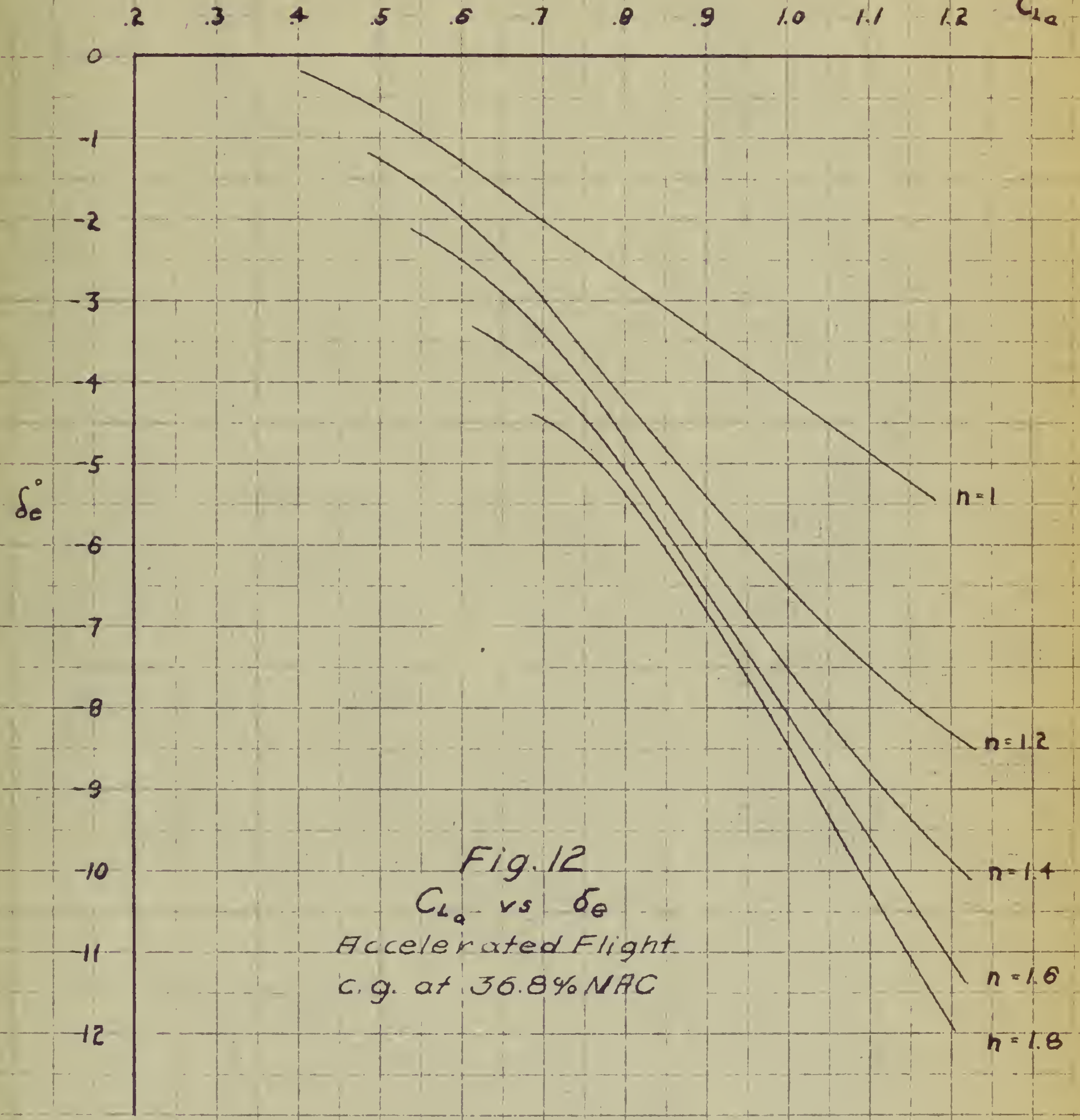

Fig. 12

C_{L_a} vs δ_e

Accelerated Flight

c.g. at 36.8% MAC

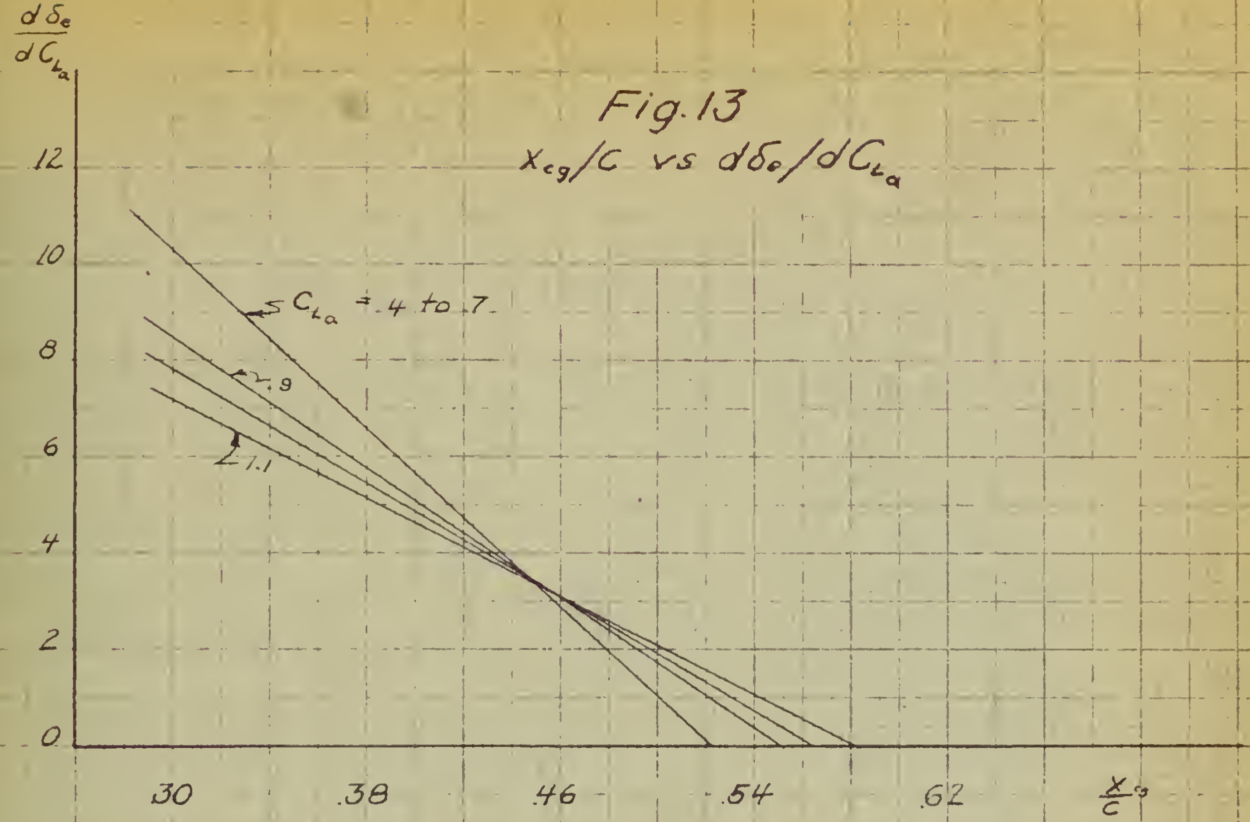

Fig. 13

x_{cg}/C vs $d\delta_e/dC_{L_a}$

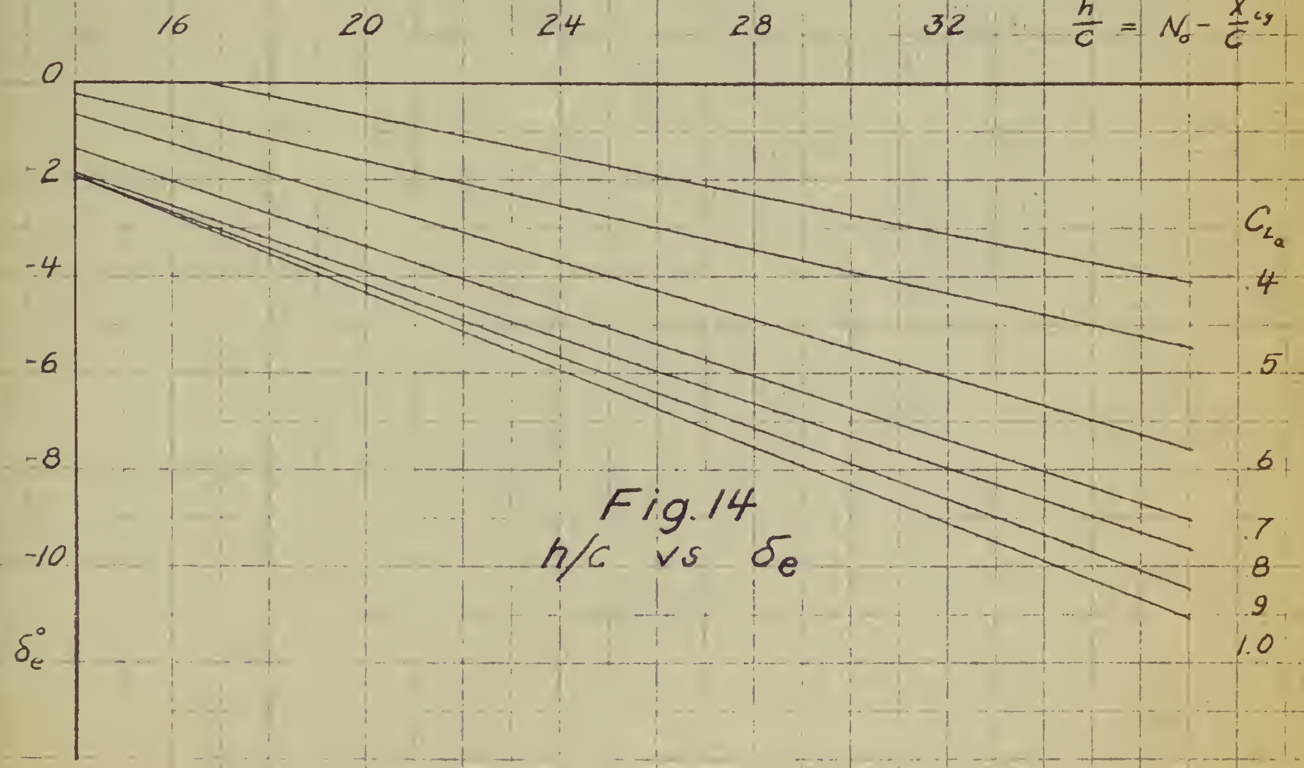

Fig. 14

h/c vs δ_e

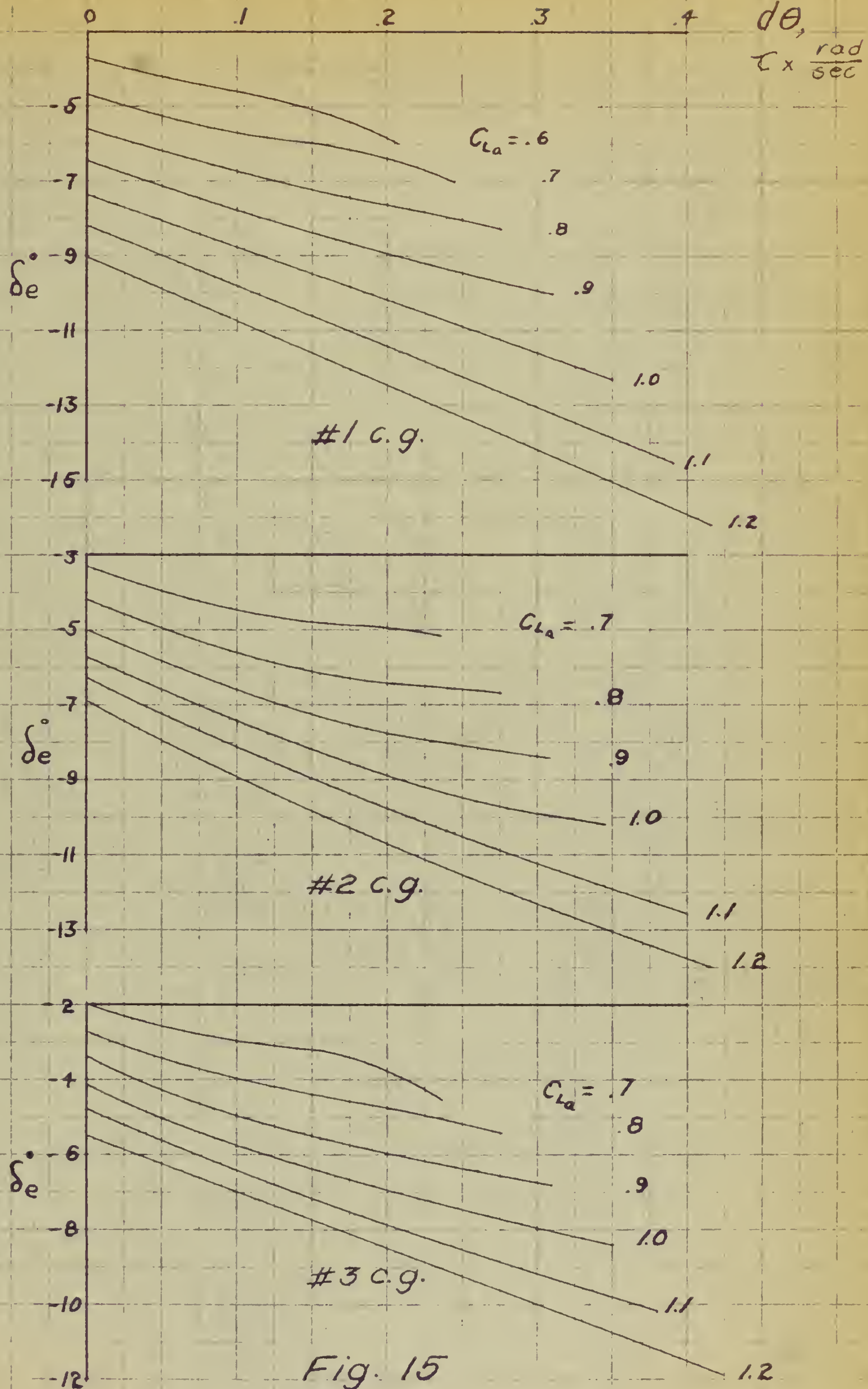

Fig. 15
dθ vs δ_e

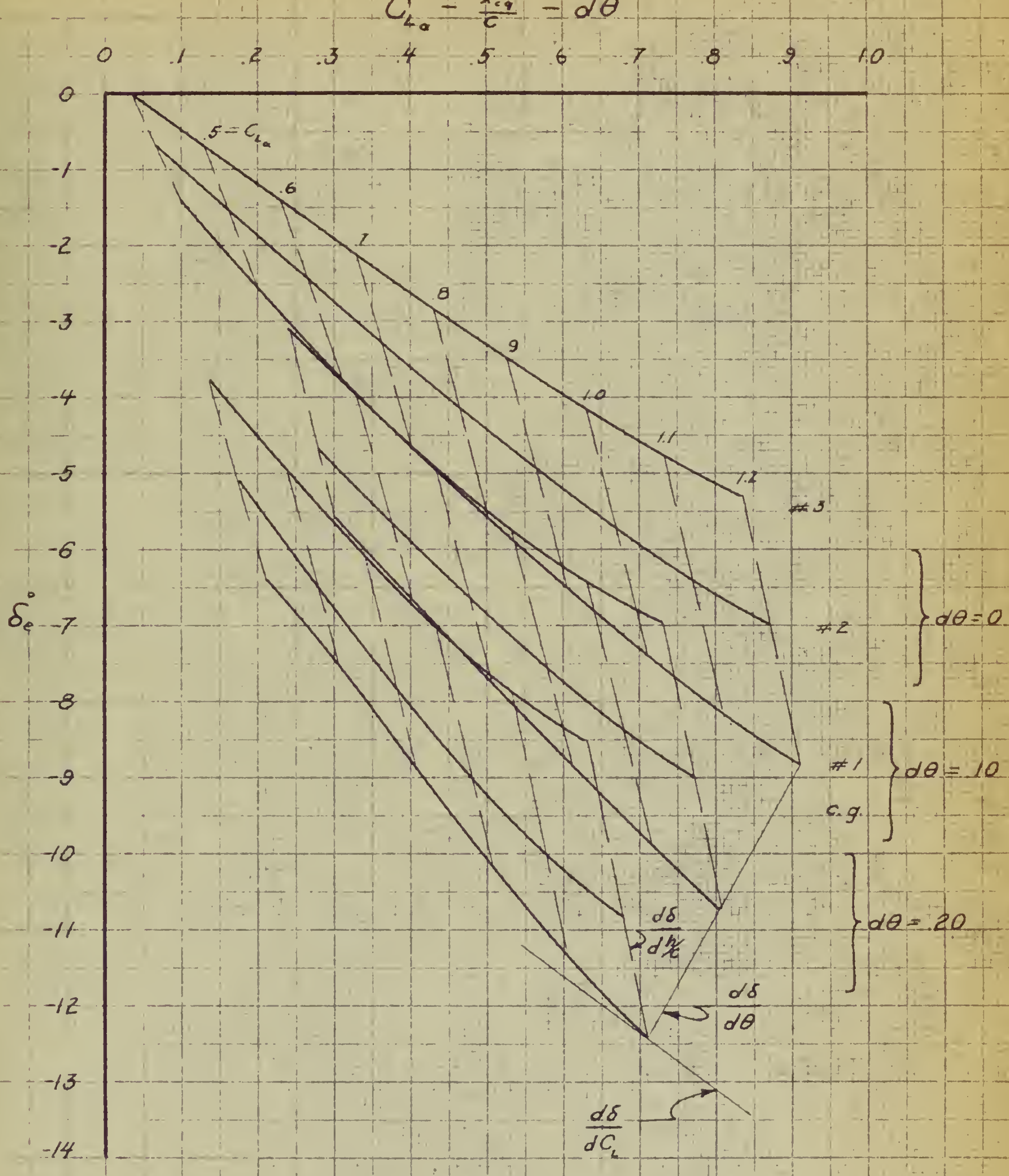

Fig. 16

$C_{L_\alpha} - x_{cg}/c - d\theta$ vs δ_e

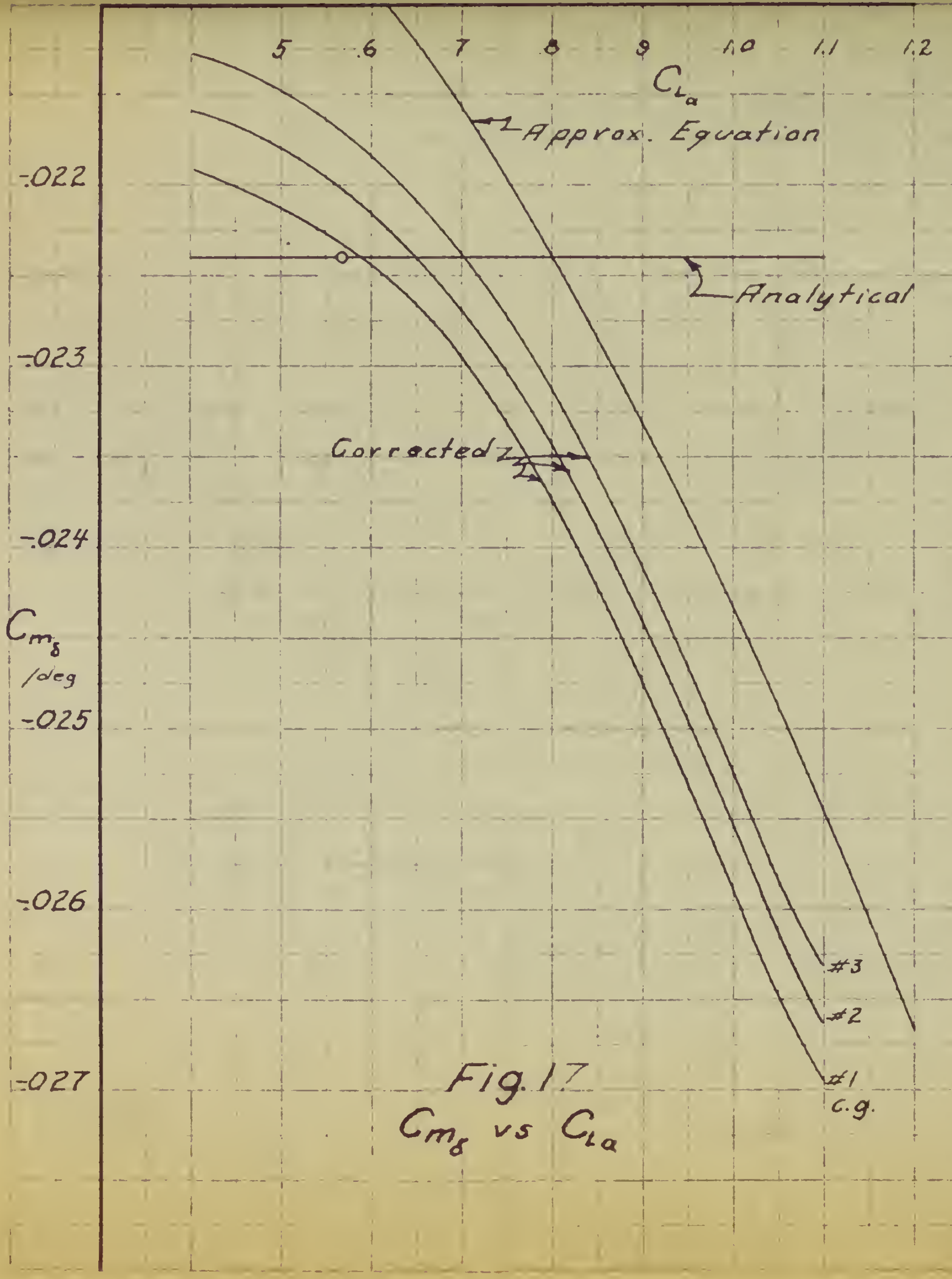

Fig. 17
C_{m_δ} vs C_{L_a}

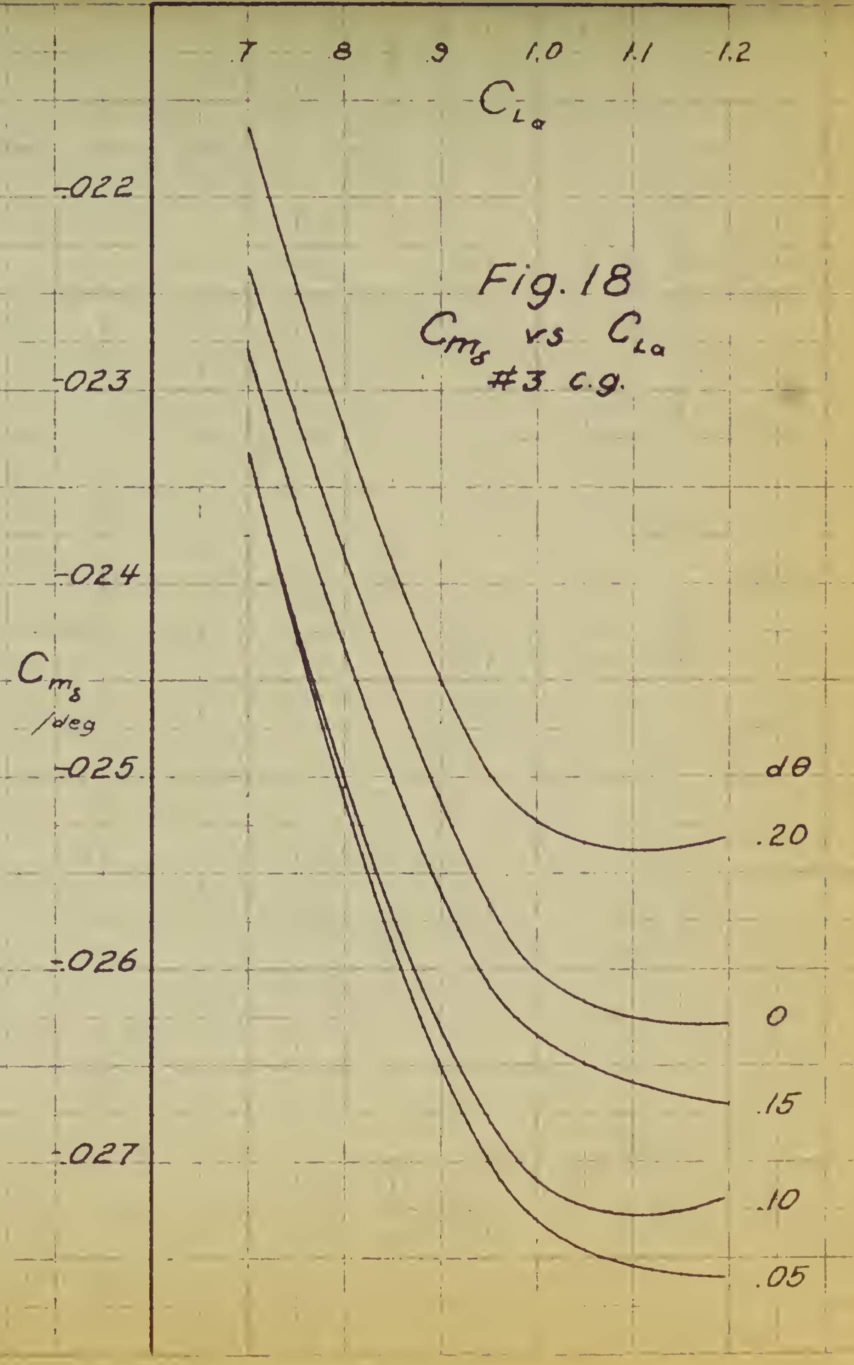

Fig. 18
C_{m_δ} vs C_{L_a}
#3 c.g.

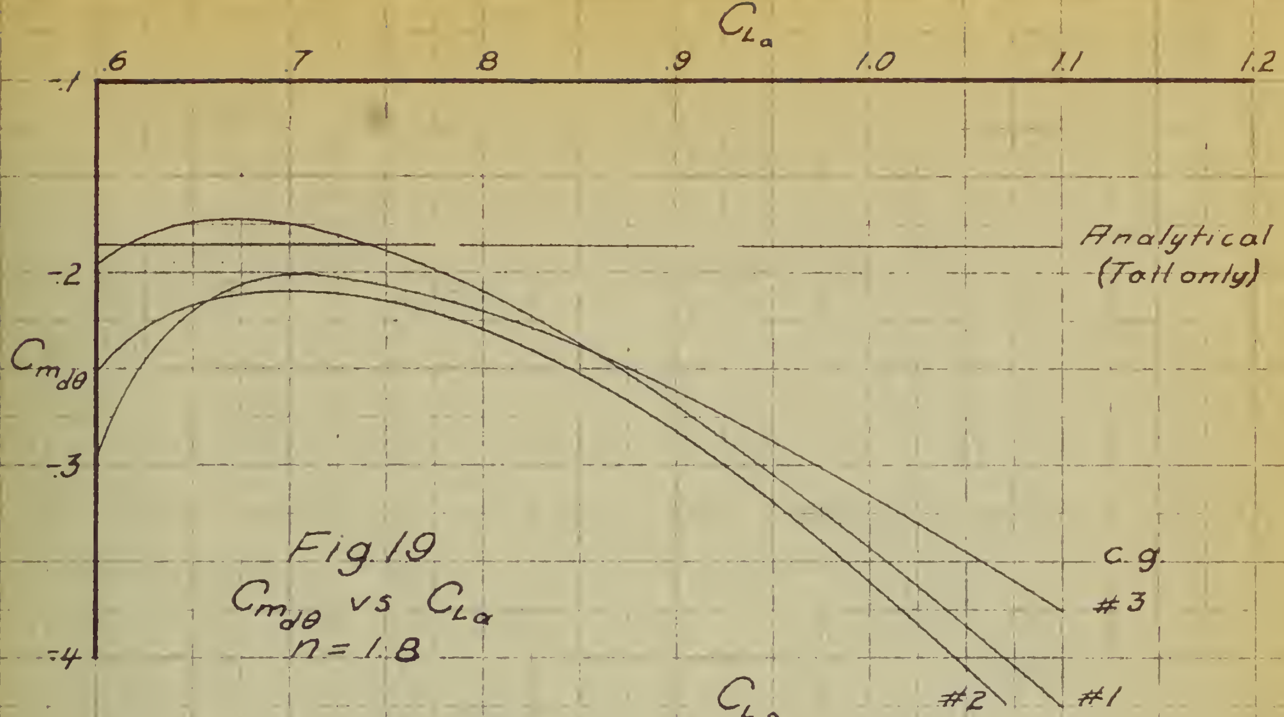

Fig. 19

$C_{m_{d\theta}}$ vs C_{L_α}

$n = 1.8$

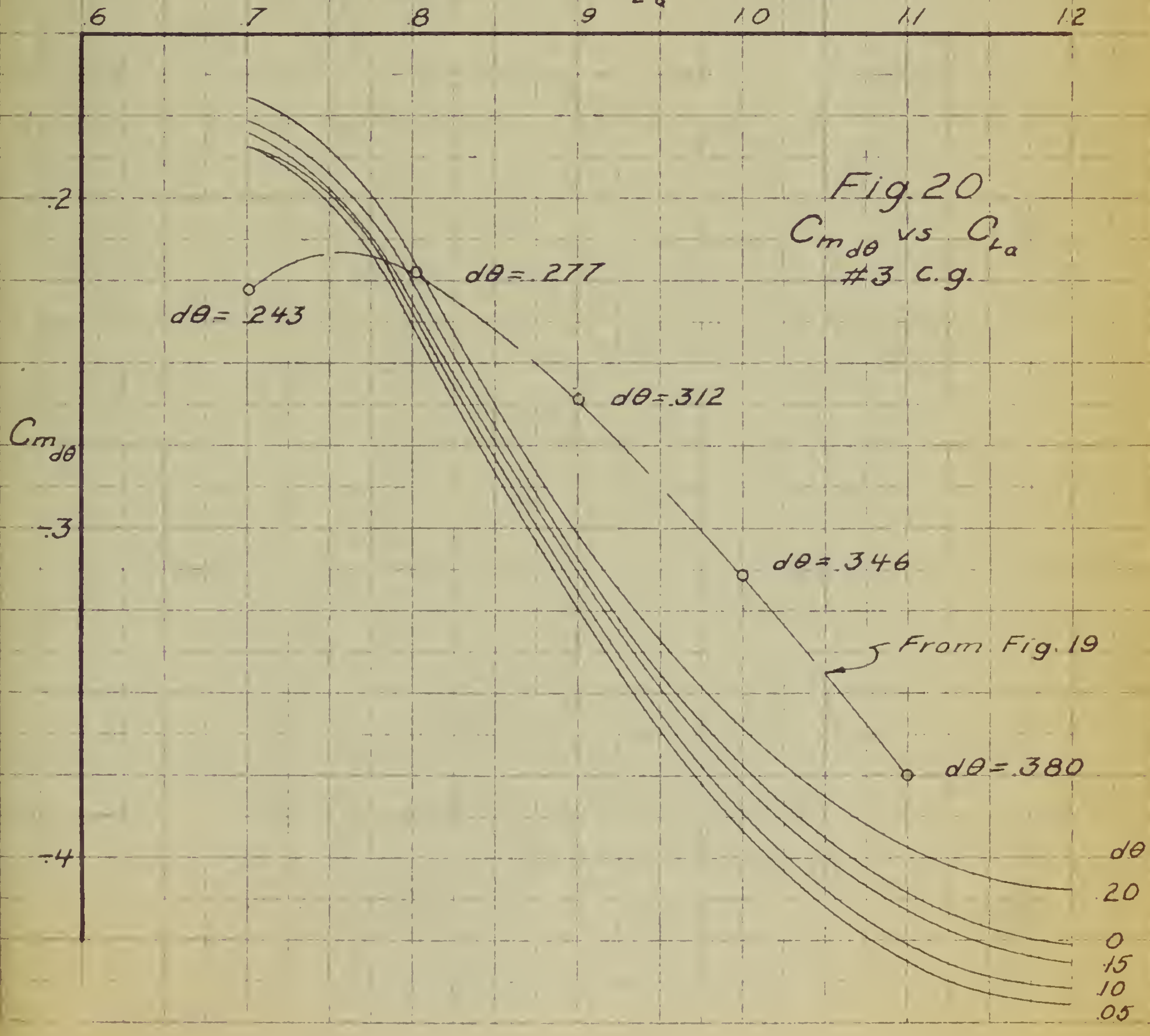

Fig. 20

$C_{m_{d\theta}}$ vs C_{L_a}

#3 c.g.

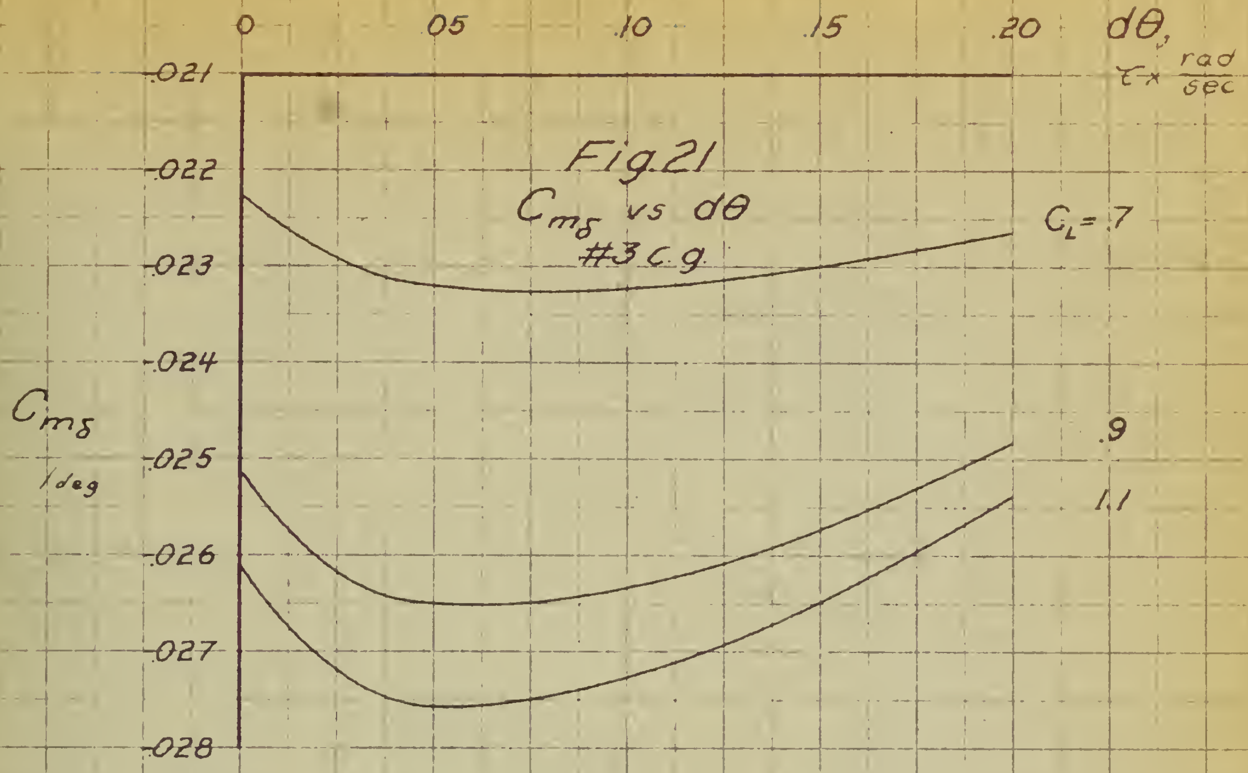

Fig.21
C_{m_δ} vs $d\theta$
#3 c.g.

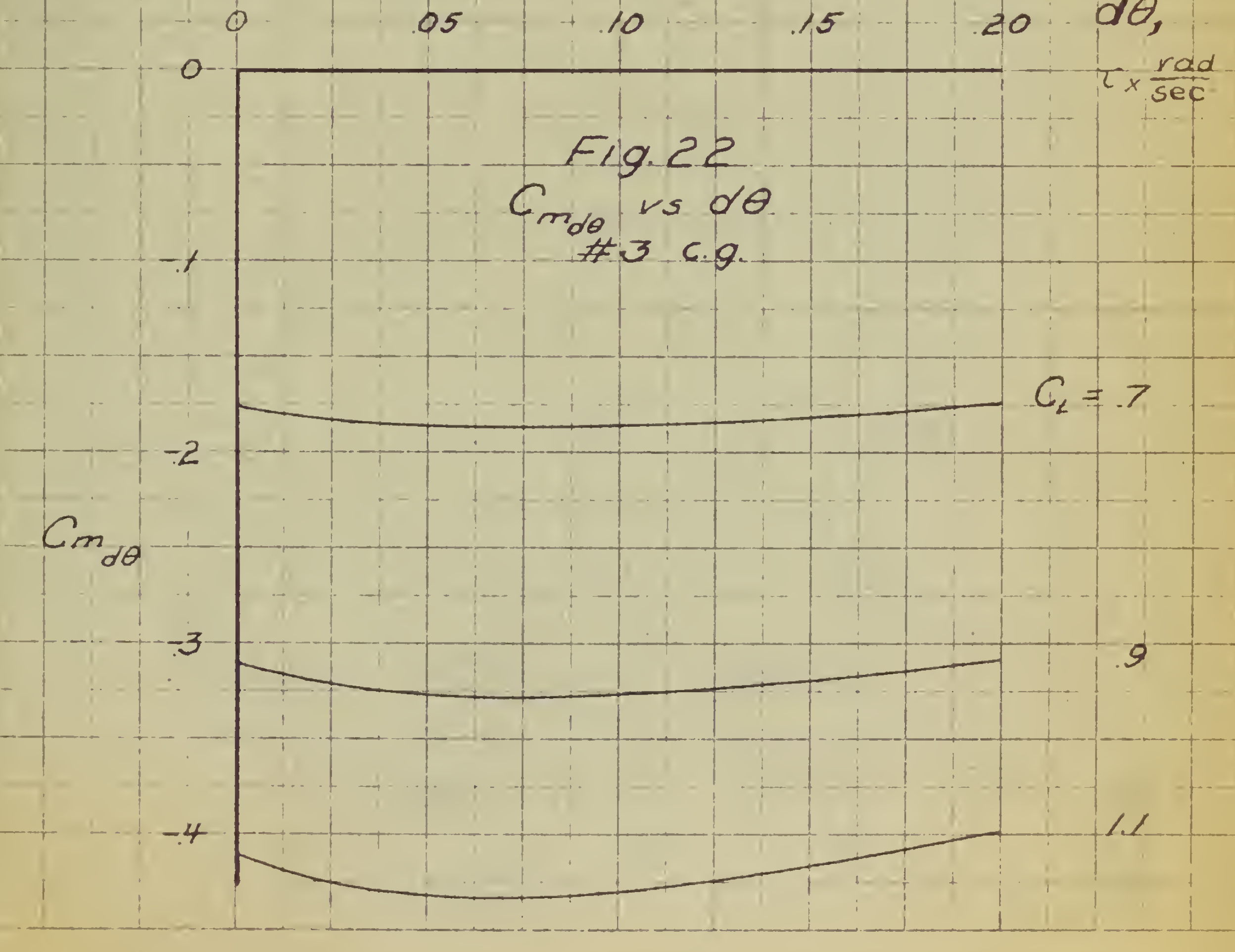

Fig. 22
$C_{m_{d\theta}}$ vs $d\theta$
#3 c.g.

Fig. 23

N_o vs C_{L_a}

#3 c.g.

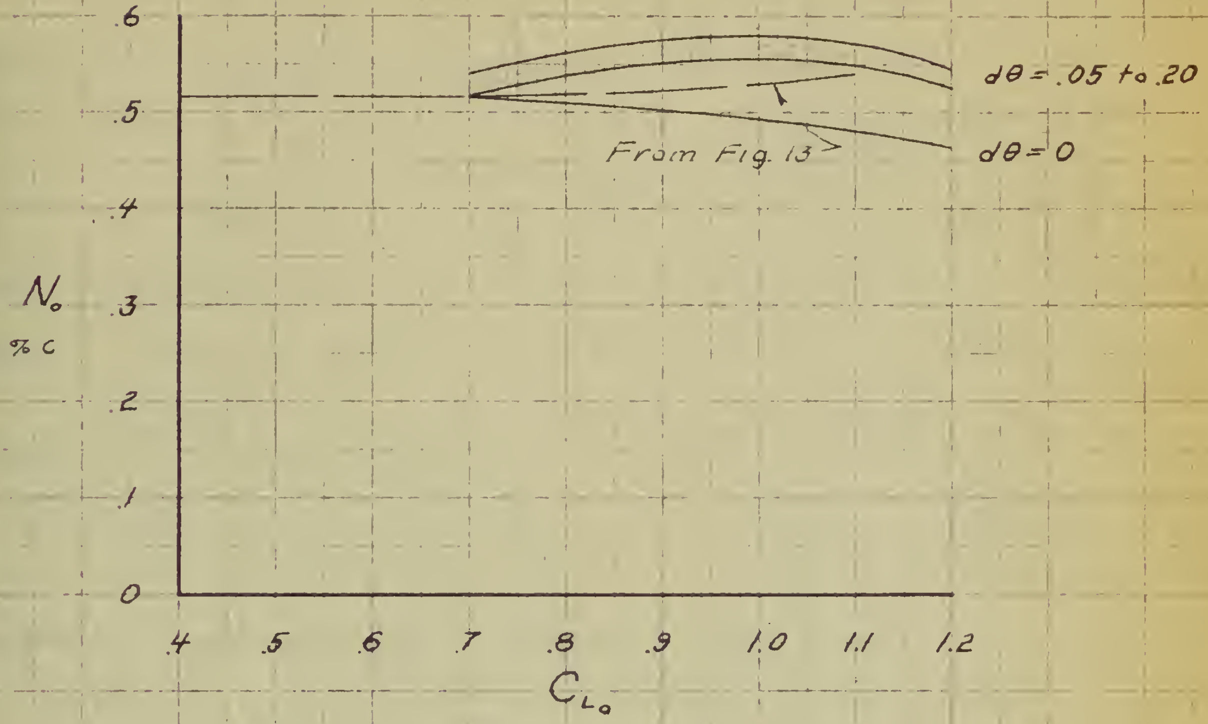

Fig. 24

N_o vs $d\theta$

#3 c.g.

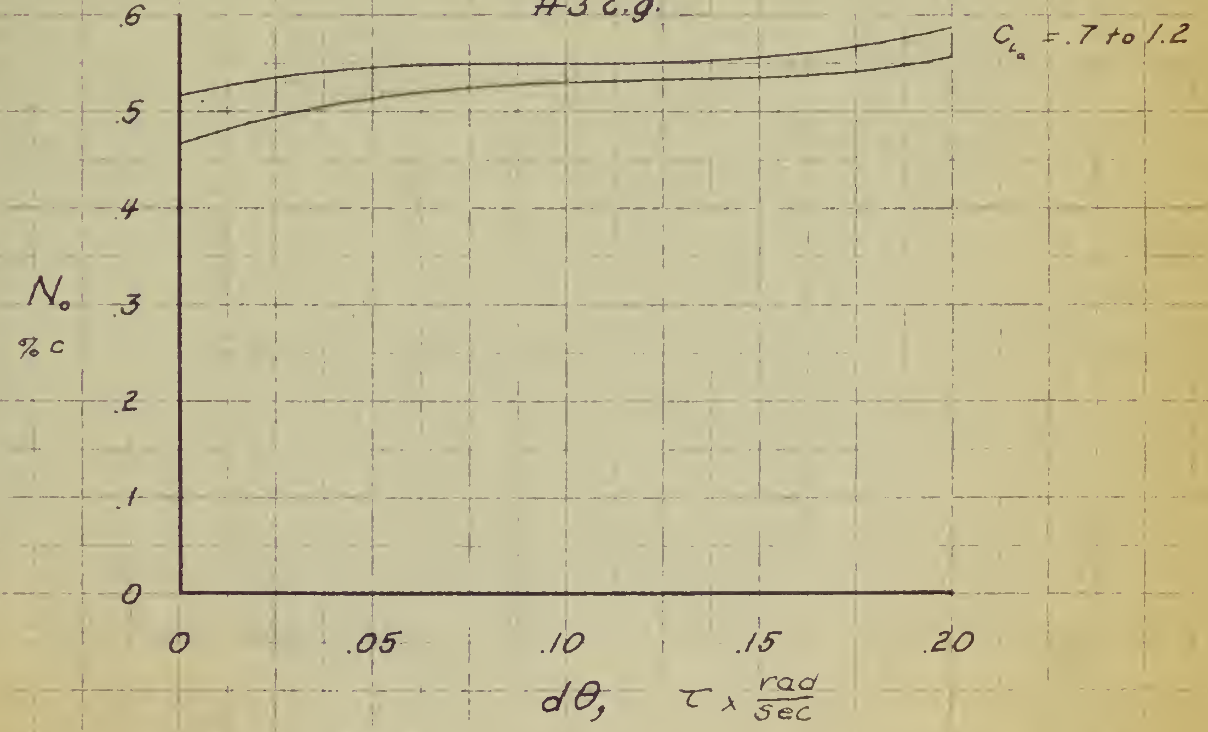

APPENDIX I

DIMENSIONS AND DESCRIPTION OF STINSON L-5 AIRPLANE

General

Manufacturer	Consolidated Vultee Aircraft Corporation
Normal Gross Weight	2200 lbs
Length (over all)	24ft. 1.25 in.
Height	10 ft. 10 in.

Wing

Airfoil Section	NACA 4412
Chord	4 ft. 9 in.
Incidence	
At Root	1° 52'
At Tip	0°
Dihedral	2° 30'
Span	33 ft. 11.4 in.
Area (total)	155 sq. ft.
Aspect Ratio	7.45

Aileron

Area	16.74 sq. ft.
Span	7 ft.
Chord	12.1 in.
Travel	
Up (from neutral)	26° 0'
Down (from neutral)	13° 2'

Stabilizer	
Area	21.8 sq. ft.
Span	11 ft. 5.5 in.
Chord	24.5 in.
Incidence	1° 30'
Elevator	
Area	13.62 sq. ft.
Travel	
Up	23° 45'
Down	23° 45'
Fin	
Area	9.71 sq. ft.
Rudder	
Area	7.05 sq. ft.
Travel	
Right	20° 0'
Left	20° 0'
Fuselage	
Maximum width	42.5 in.
Maximum height	66.0 in.
Engine	
Type	Lycoming 0-435-1

APPENDIX II

WEIGHT AND BALANCE COMPUTATIONS

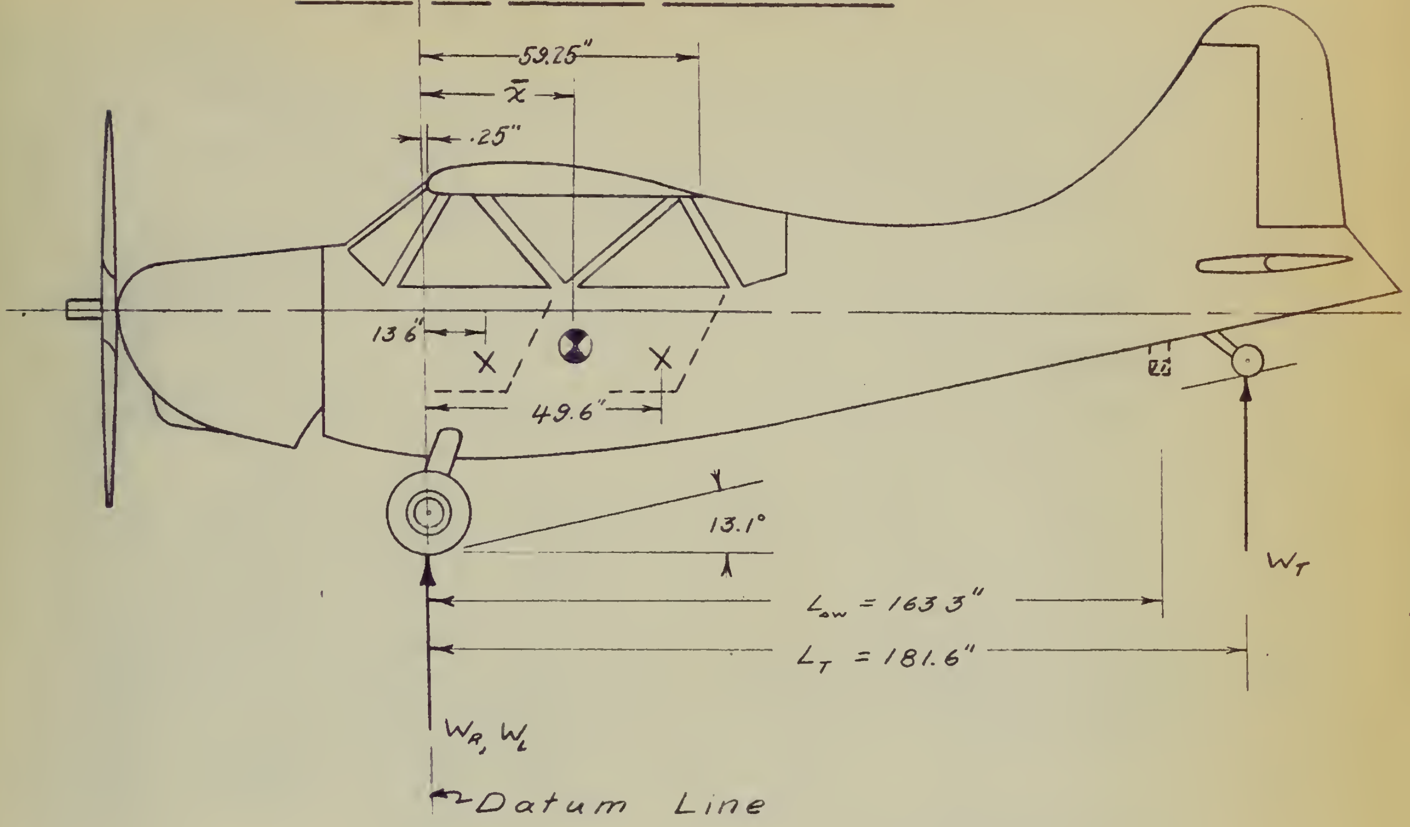

Condition: Oil and fuel tanks full.
Test equipment installed except as indicated.

1. **Weight**: (Airplane weighed in level flight attitude.)

Scale No.	Wheel	Gross Weight	Tare	Net Weight
F263110	Left	869#	1.5#	867.5#
F263111	Right	867#	2.5#	864.5#
-	Tail	137#	1.5#	135.5#
				1867.5#

Pilot & Parachute	180#	
Observer & Parachute	210#	
	390#	
Airplane Take-Off Weight		2257.5#

2. **Balance:**

Datum line (reference)	main gear axel
Wing chord (MAC)	57.00"
Root leading edge to datum line	0.25"
Datum line to tail wheel	181.60"
Datum line to pilot	13.60"
Datum line to observer	49.60"

$$\bar{x} = \frac{W_T \times L_T + W_{Pilot}\, L_{Pilot} + W_{Obs.}\, L_{Obs.}}{W_{T.O.} - W_{Fuel\ Used}}$$

$$\bar{x}_{c.g.} = \bar{x} - 0.25''$$

No account was made for minor moments due the airplane c.g. shift with respect to the c.g. of the fuel tanks since the fuel tanks were located longitudinally at the mid-c.g. position.

(a) Forward c.g. position: (#1 c.g.)

$$\bar{x}_{c.g\#1} = \frac{135.5\# \times 181.6'' + 180\# \times 13.6'' + 210\# \times 49.6''}{2257.5\# - W_{Fuel\ Used}}$$

$$= 37{,}470.8/2233.5 = 16.78''$$

$$\left(\frac{\bar{x}}{c}\right)_{c.g\#1} = \frac{16.78'' - 0.25''}{57''} = 0.290$$

(b) Mid - c.g. position: (#2 c.g.)

$$\bar{x}_{c.g\#2} = \frac{37{,}470.8 + \Delta W \times L_{\Delta W}}{2257.5 + \Delta W - W_{Fuel\ Used}}$$

$$= \frac{37{,}470.8 + 36.06\# \times 163.3''}{2257.5\# + 36.06 - W_{Fuel\ Used}}$$

$$= 43{,}358.8/2269.5 = 19.10''$$

$$\left(\frac{\bar{x}}{c}\right)_{c.g\#2} = \frac{19.10'' - 0.25''}{57''} = 0.331$$

(c) Aft c.g. position: (#3 c.g.)

$$\bar{x}_{c.g.\#3} = \frac{37,470.8 + 69.62\# \times 163.3''}{2257.5 + 69.62 - W_{Fuel\ Used}}$$

$$= 48,839.7/2303.1 = 21.20''$$

$$\left(\frac{\bar{x}}{c}\right)_{c.g.\#3} = \frac{21.20'' - 0.25''}{57''} = 0.368$$

Miscellaneous:

Drogue sleeve	3#
Complete drag measuring equipment and fittings	13#
Wing weight and fittings	30# 9oz
Dummy weight and fittings	1# 9oz

APPENDIX II

LIST OF SYMBOLS AND CONVENTIONS

V_e	Equivalent airplane speed (mph)
V	True airspeed (fps)
W	Airplane weight (lbs)
S	Wing area (sq. ft.)
b	Wing span (ft)
c'	Mean aerodynamic chord (ft)
S_t	Tail area (sq. ft.)
l_t	Tail length (c.g. to aerodynamic center of horizontal tail) (ft)
$\overline{V}$	Tail volume coefficient ($S_t l_t / S_w c$)
l_v	Tail length (c.g. to aerodynamic center of vertical tail) (ft)
h_v	Vertical tail centroid to X-axis (ft)
x_a/c	Chord lengths of c.g. aft of wing leading edge (ft)
h/c	Chord lengths of c.g. fwd of a.c. (ft)
δ_e	Elevator angle (degrees)
δ_a	Aileron angle (degrees)
δ_r	Rudder angle (degrees)
β	Sideslip angle (degrees)
ψ	Yaw angle (degrees)
ϕ	Bank angle (degrees)
$\dot{\psi}$	Time rate of yaw (degrees/sec)
C_{L_a}	Airplane lift coefficient
C_{L_W}	Wing lift coefficient

a_t	Slope of horizontal tail lift curve
a_v	Slope of vertical tail lift curve
a_w	Slope of wing lift curve
q	Dynamic pressure (lbs/sq ft)
n	Normal acceleration in units of "g"
g	Acceleration of gravity (32.2 ft/sec^2)
η_t	Tail efficiency factor
τ_e	Elevator effectiveness $\left(\frac{d\alpha_t}{d\delta_e}\right)$
τ	Airplane time characteristic $m/\rho S V$
μ	Airplane relative density $m/\rho S c$
θ	Angle of pitch
d	Operator $\frac{d}{d(t/\tau)}$
$C_{n_{\delta_e}}$	Elevator control power derivative
$C_{m_{d\theta}}$	Damping in pitch derivative
C_{y_β}	Side force derivative
Cn_β	Directional stability derivative
C_{l_β}	Dihedral effect derivative
C_{n_r}	Yaw damping derivative
$C_{n_{\delta_r}}$	Rudder control power derivative
$C_{l_{\delta_a}}$	Aileron control power derivative
$C_{y_{\delta_r}}$	Side force due to derivative
C_{l_p}	Roll damping derivative
$C_{l_{\delta_r}}$	Secondary rudder derivative
$C_{n_{\delta_a}}$	Secondary aileron derivative

Axis system and convention used: (see Ref. 1, page 376)

Appendix IV
Strain Gauge

Bridge & Network

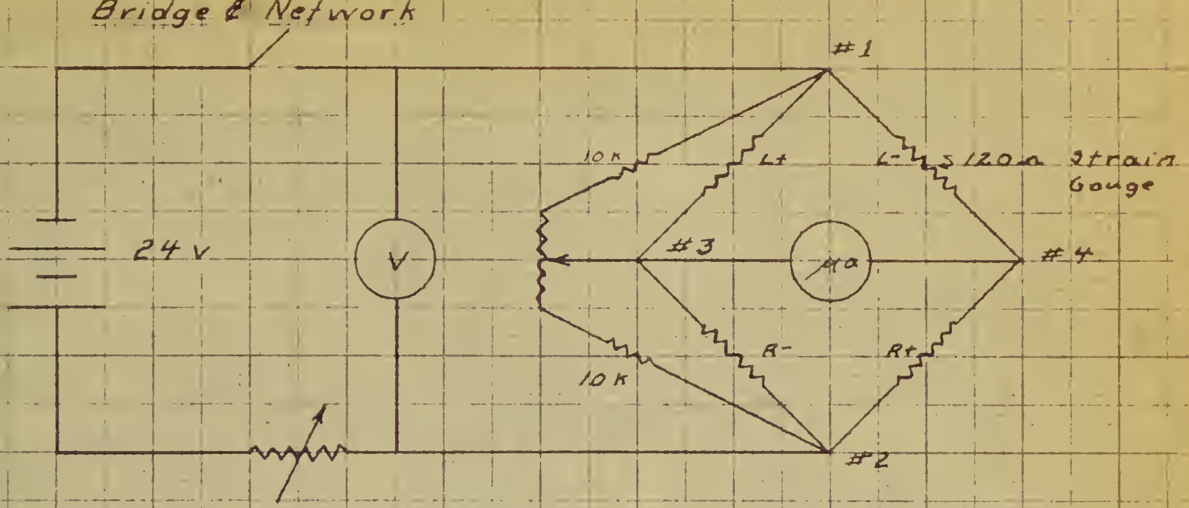

Strain Gauge

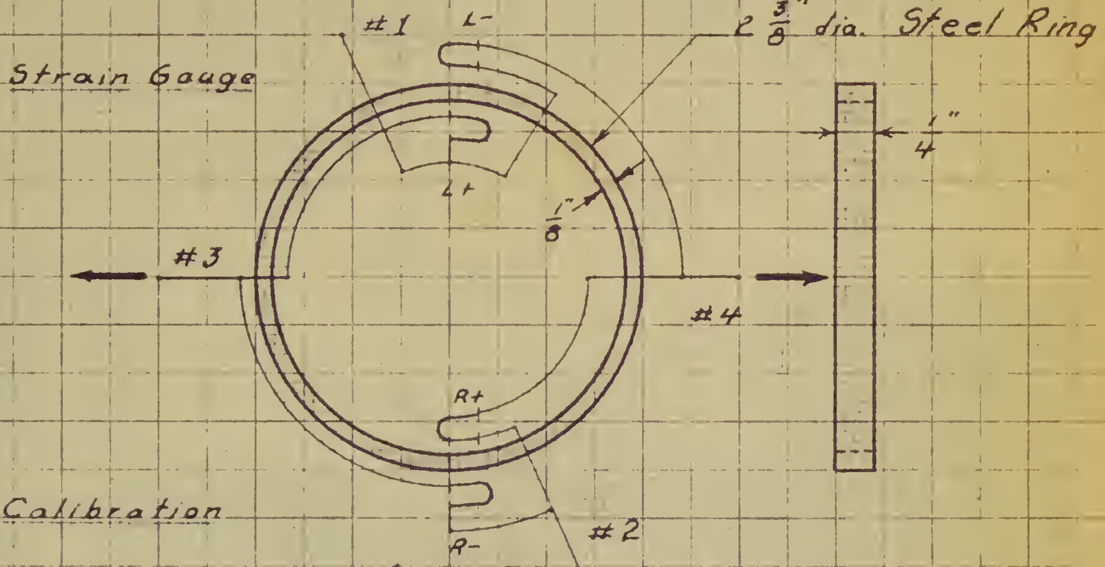

Calibration

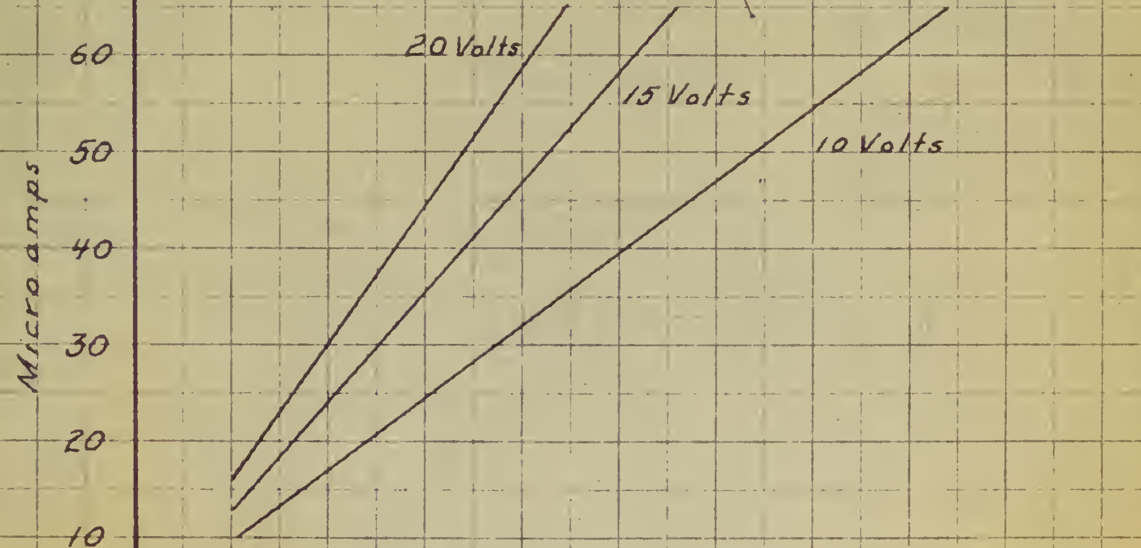

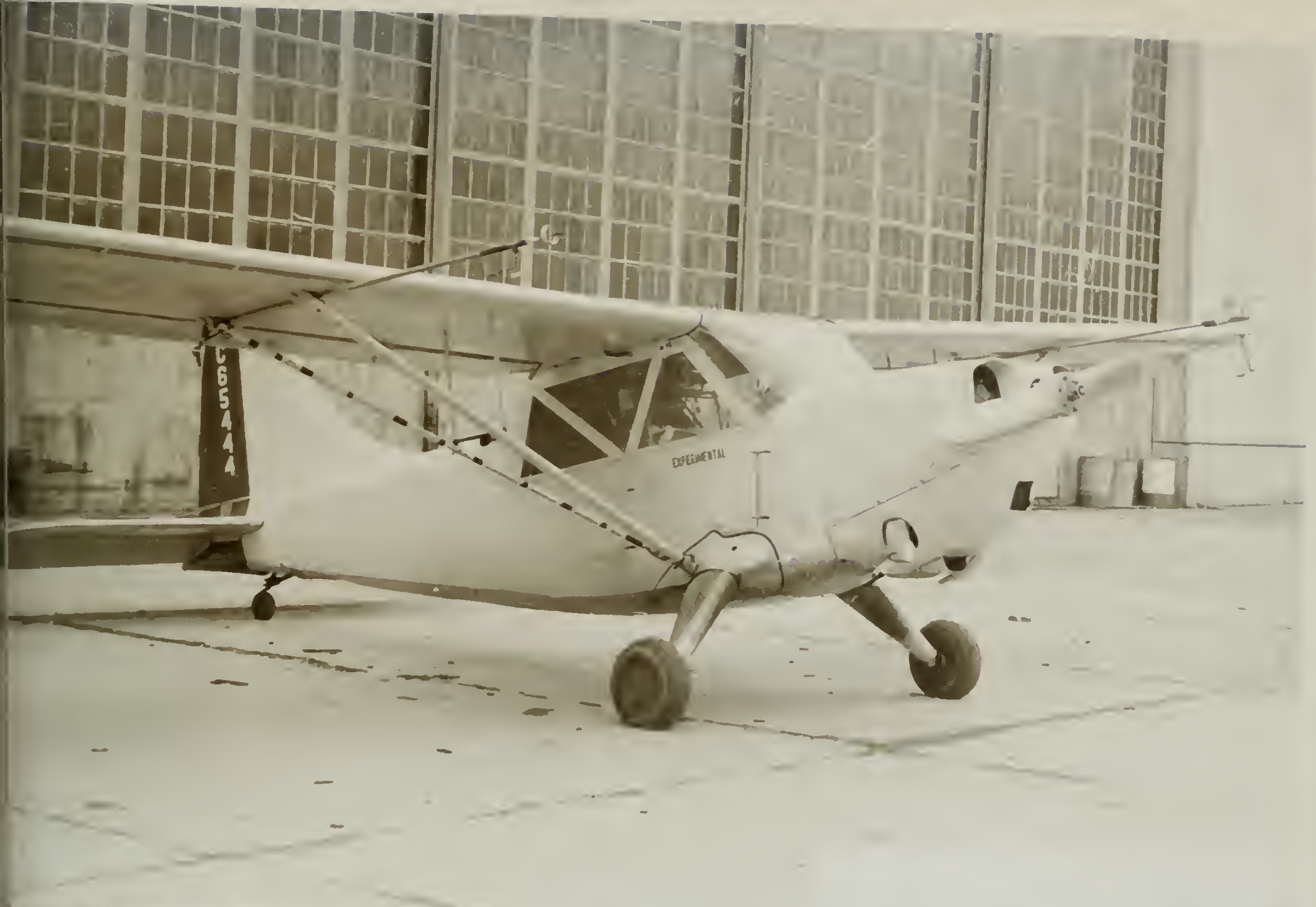

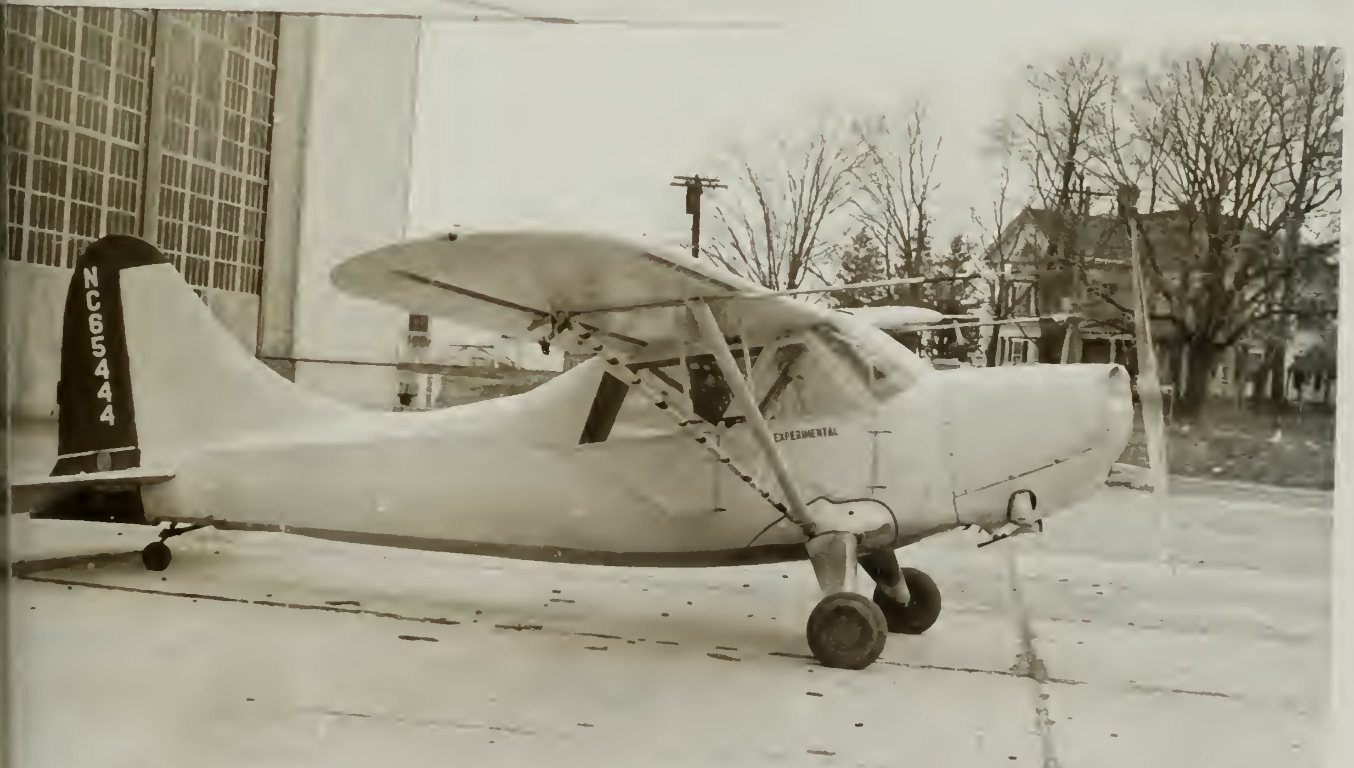

Appendix V

707

MY 16 62 11646
NO 20 62 11146

Thesis 18196
S 153

Saldin
Determination of the longitudinal and lateral stability derivatives of the Stinson L-5 airplane

MY 16 62 11646
NO 20 62 11146

96

Thesis 18196
S153

Saldin

Determination of the longitudinal and lateral stability derivatives of the Stinson L-5 airplane from steady state flight tests.

Library
U. S. Naval Postgraduate School
Monterey, California

thesS153
Determination of the longitudinal and la
3 2768 001 97698 8
DUDLEY KNOX LIBRARY